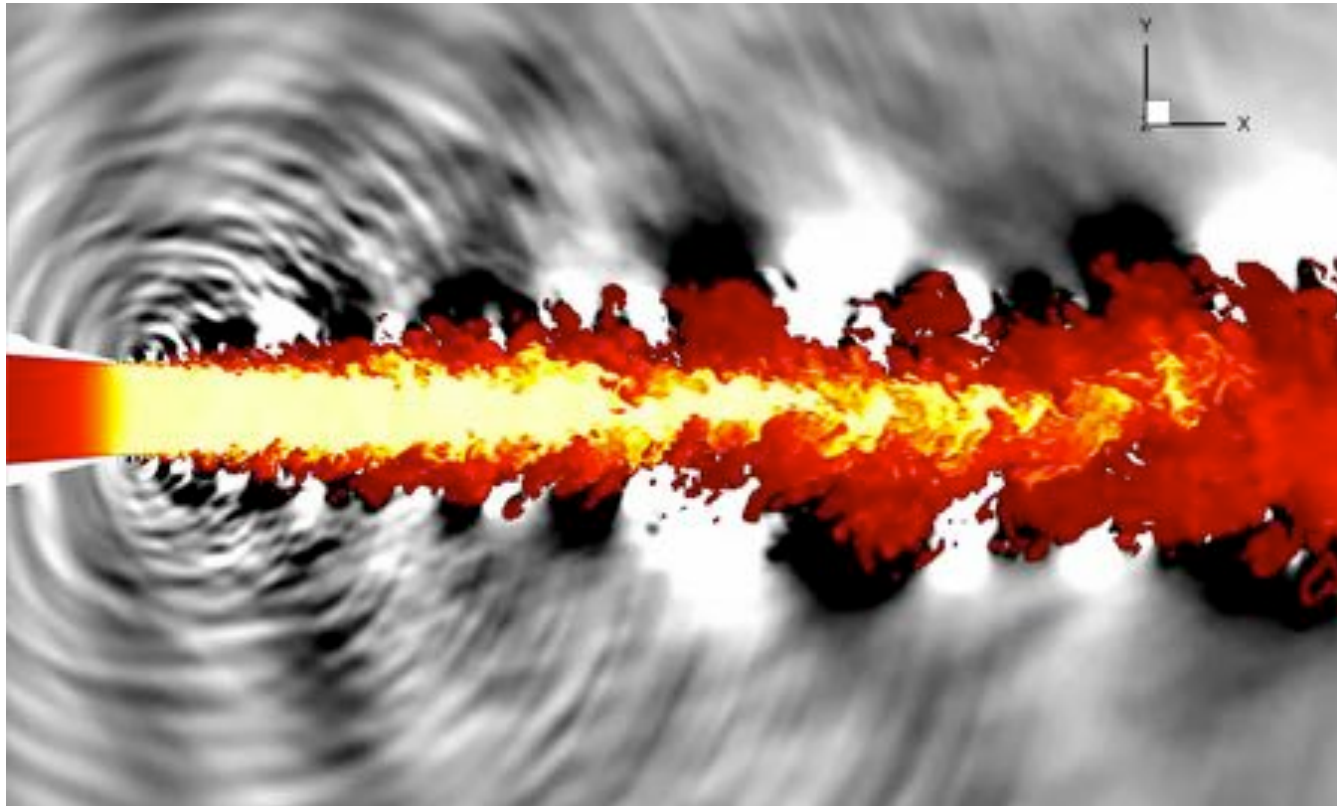


# Jet Noise Prediction using Hybrid RANS/LES with Structured Overset Grids



**Jeffrey Housman**

**Computational Aerosciences Branch**

**NASA Ames Research Center**

**Co-Researchers: Gerrit-Daniel Stich, Cetin Kiris, and James Bridges**

**Advanced Modeling & Simulation Seminar Series**

**NASA Ames Research Center, September 28, 2017**

**AIAA-2017-3213: J. Housman, G. Stich, C. Kiris, J. Bridges**

# Outline

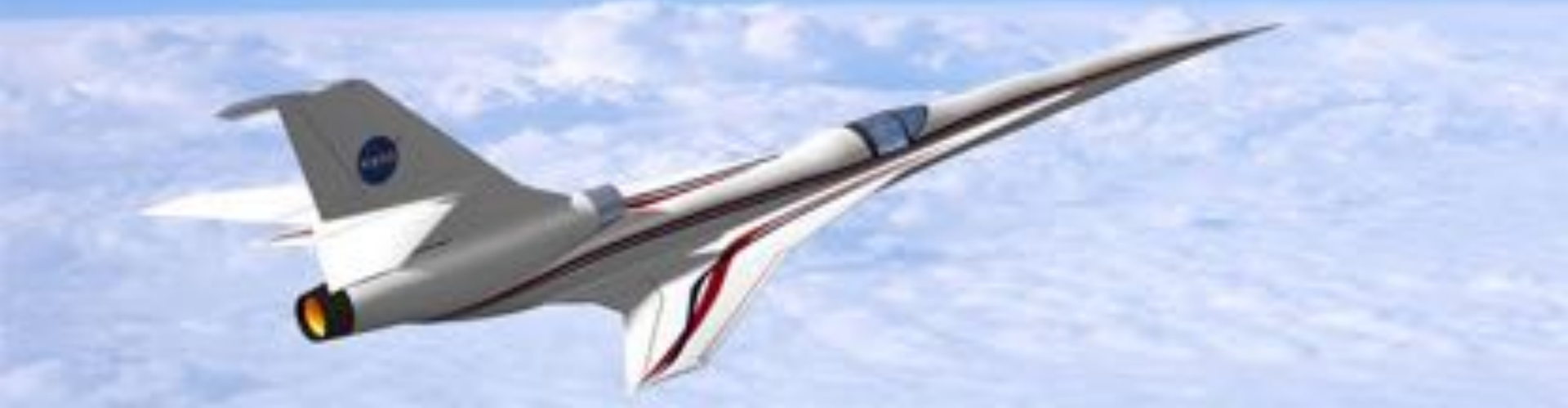


- Introduction
- Experimental Setup
- Computational Methodology
- Structured Overset Grid System
- Computational Results
  - Near-Field Comparison
  - Far-Field Comparison
- Summary
- Future Work

# Introduction



Commercial Supersonic Transport (CST) ; Advanced Air Vehicle Program (AAVP)

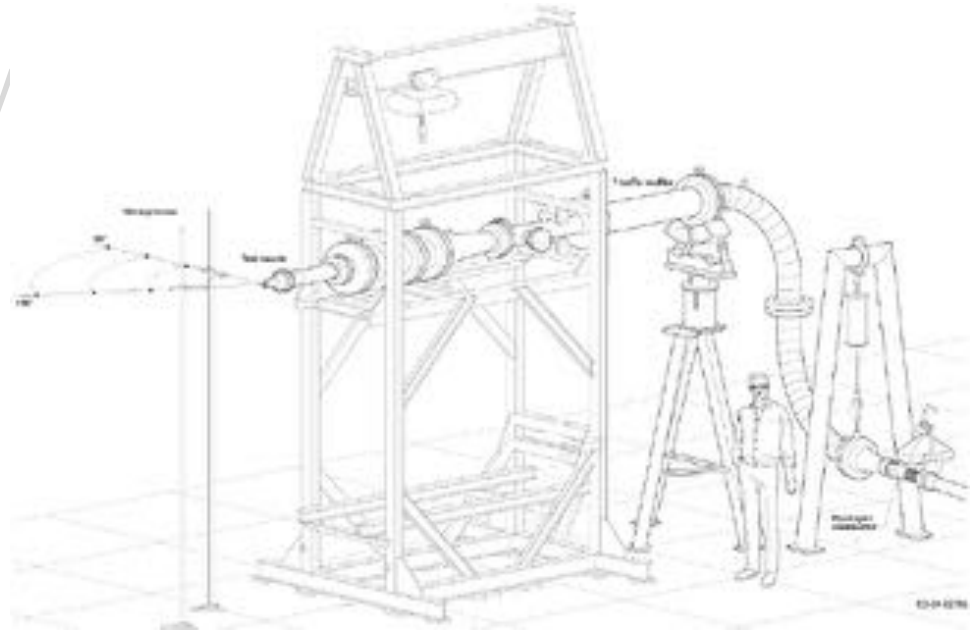


- NASA has initiated research activities toward quiet supersonic flight.
- Reduction of sonic boom ground signature.
- Constraints during takeoff and landing at subsonic speeds must be satisfied.
- Use computational aeroacoustics (CAA) tools to assess new designs.
- First part of a systematic validation effort in jet noise prediction capability for NASA Ames Launch Ascend and Vehicle Aerodynamics Code (LAVA).

# Outline



- Introduction
- **Experimental Setup**
- Computational Methodology
- Structured Overset Grid System
- Computational Results
  - Near-Field Comparison
  - Far-Field Comparison
- Summary
- Future Work

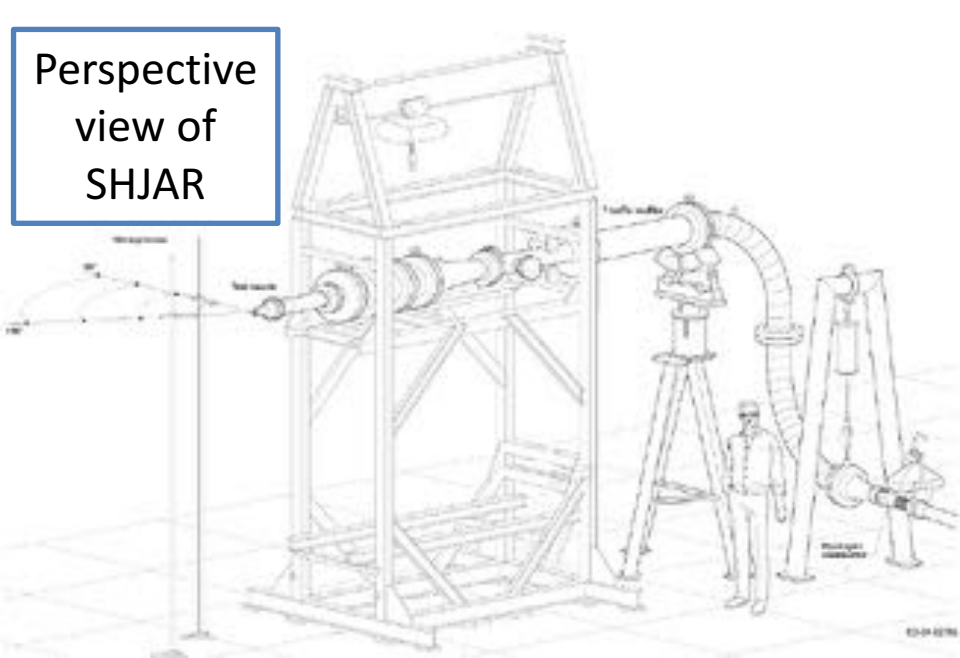


# Experimental Setup

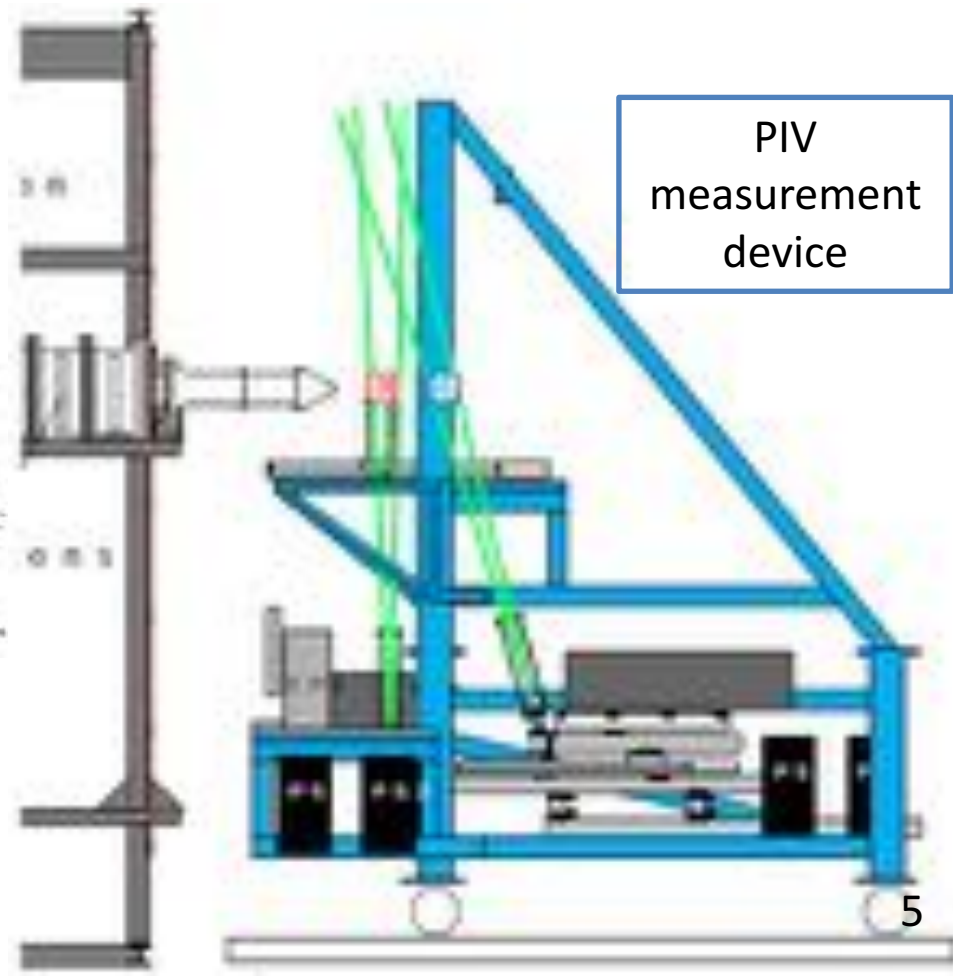


- Small Hot Jet Acoustic Rig (SHJAR), which is located in the Aeroacoustics Propulsion Lab (AAPL) at NASA Glenn Research Center

Perspective  
view of  
SHJAR



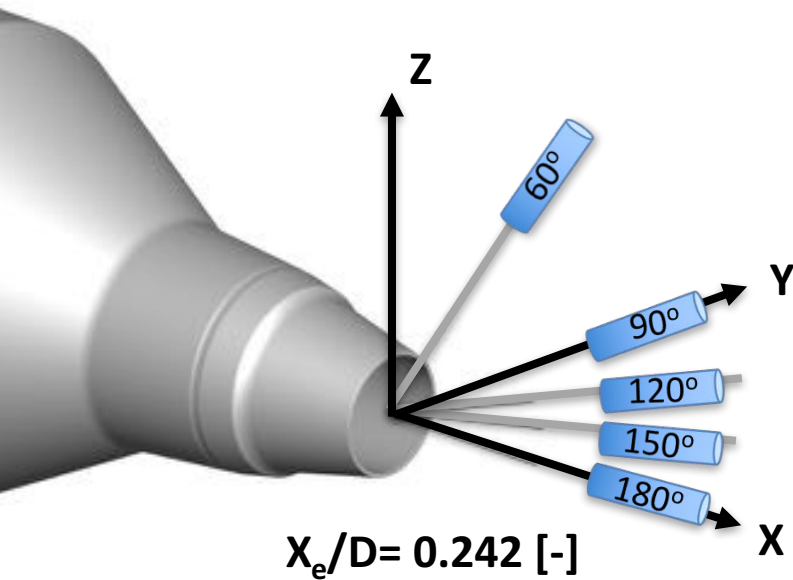
PIV  
measurement  
device



Bridges et. al. (NASA-TM-2011-216807)

# Experimental Setup

- Baseline axisymmetric convergent Small Metal Chevron (SMC000) nozzle at Set Point 7 (SP7)
- Nozzle axis in downstream flow direction is marked as 180°

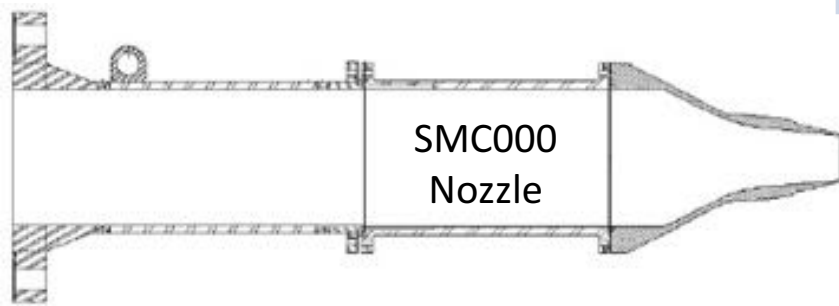


Bridges et. al. (NASA-TM-2011-216807)	SP7
Acoustic Mach number $U_{jet}/c_\infty$	0.9
Jet temperature ratio $T_e/T_\infty$	0.835
Nozzle pressure ratio $p_t/p_\infty$	1.861
Nozzle Diameter D	0.0508 [m] 2.0 [inch]
Reynold number $Re_D$	1 Million
Reynolds number $Re_\tau$	800
Boundary layer thickness	0.0128 D

similar to: Bres et. al. (AIAA-2015-2535)

“Bruit et vent” jet-noise facility at

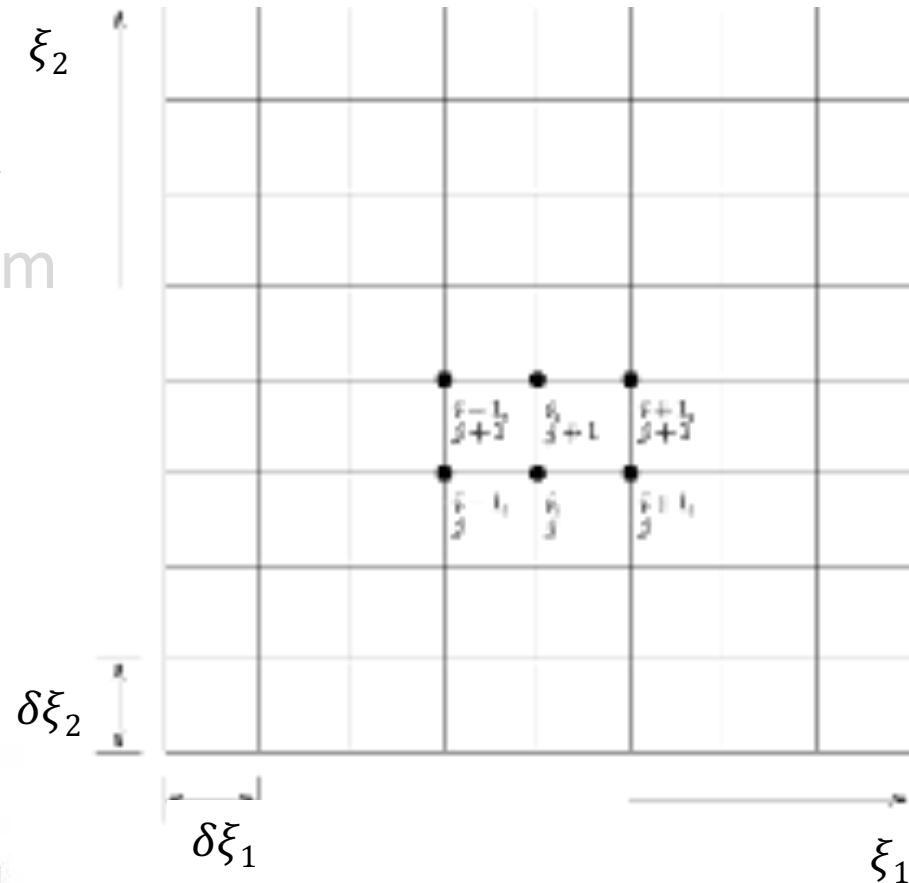
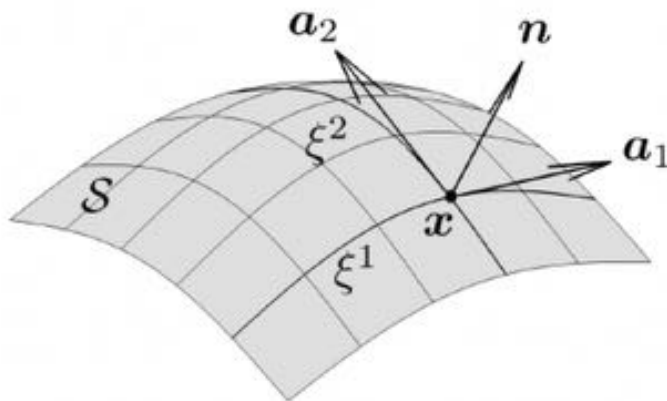
Centre d’Etudes Aerodynamique et Thermique



# Outline



- Introduction
- Experimental Setup
- **Computational Methodology**
- Structured Overset Grid System
- Computational Results
  - Near-Field Comparison
  - Far-Field Comparison
- Summary
- Future Work



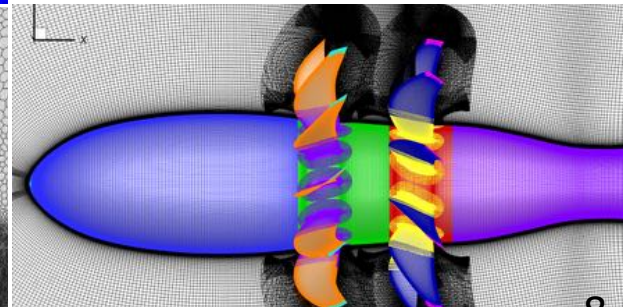
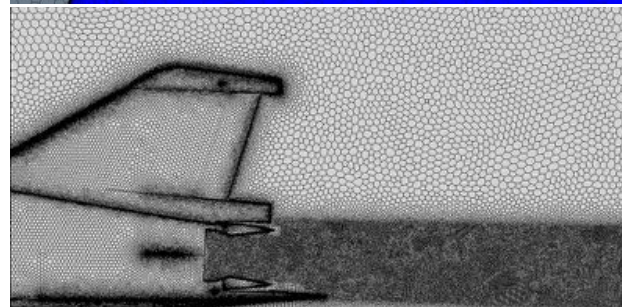
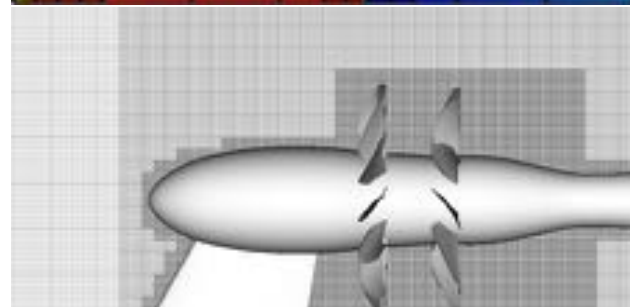
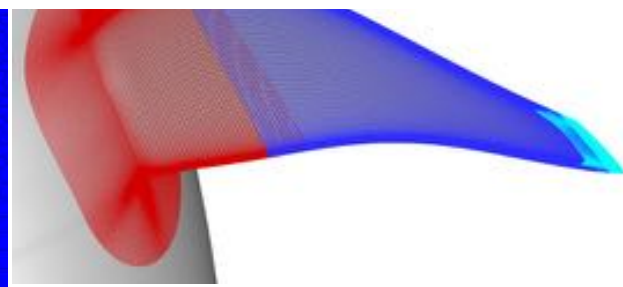
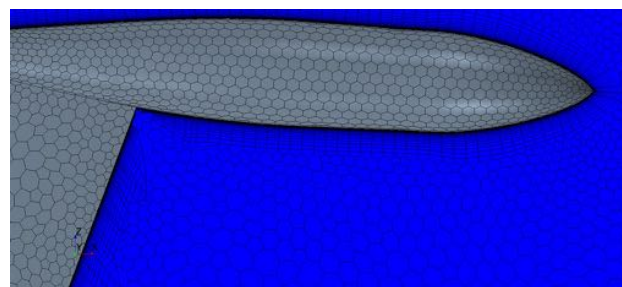
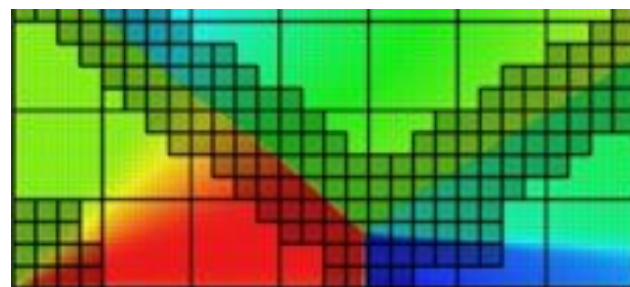


# Computational Methodology



## *LAVA Framework* (Kiris et al. Aerospace Science and Technology, Volume 55, 2016)

- Computational Fluid Dynamics Solvers
  - Cartesian, Curvilinear, and Unstructured Grid Types
  - Overset Grid and Immersed Boundary Methods
  - Steady and Unsteady RANS (Reynolds-Averaged Navier-Stokes)
  - Hybrid RANS/LES (Large Eddy Simulation), LES and LBM Capabilities
- Acoustic Solver
  - Linear Helmholtz Scattering Code
  - Permeable Surface Flow Williams-Hawkins Propagation (FWH)



***Cartesian Immersed Boundary***

***Unstructured Arbitrary Polyhedral***

***Overset Structured Curvilinear***



# Computational Methodology

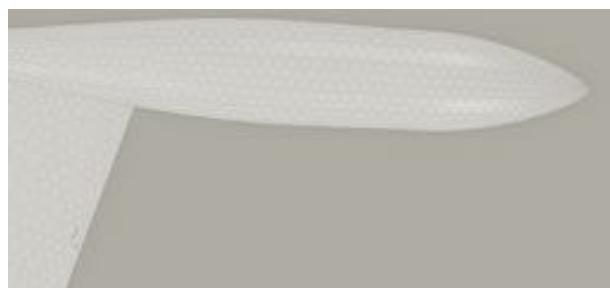


## *LAVA Framework* (Kiris et al. Aerospace Science and Technology, Volume 55, 2016)

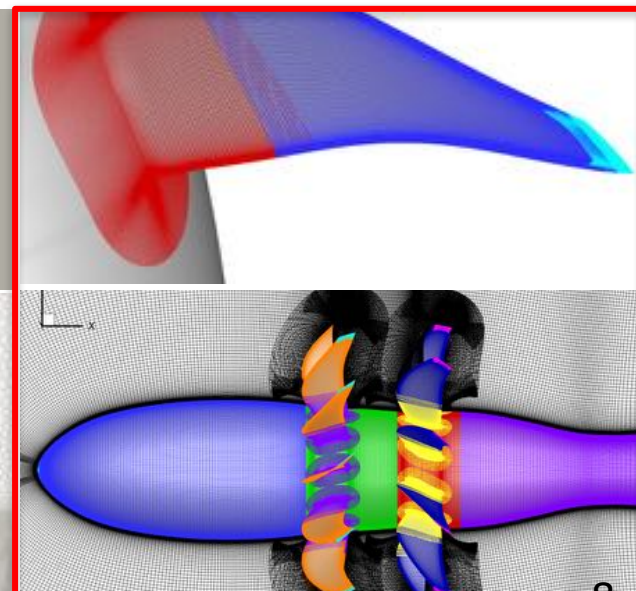
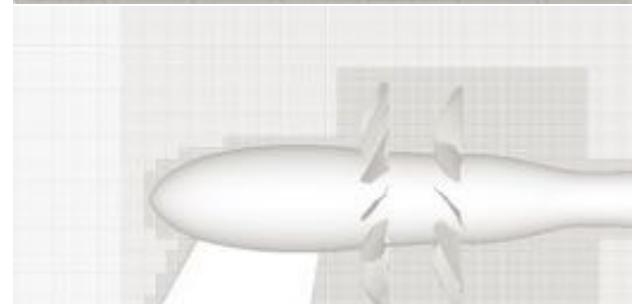
- Computational Fluid Dynamics Solvers
  - Cartesian, **Curvilinear**, and Unstructured Grid Types
  - **Overset Grid** and Immersed Boundary Methods
  - Steady and **Unsteady RANS** (Reynolds-Averaged Navier-Stokes)
  - **Hybrid RANS/LES** (Large Eddy Simulation), LES and LBM Capabilities
- Acoustic Solver
  - Linear Helmholtz Scattering Code
  - **Permeable Surface Ffowcs Williams-Hawkings Propagation (FWH)**



*Cartesian Immersed Boundary*



*Unstructured Arbitrary Polyhedral*



*Overset Structured Curvilinear*

## *3-D Structured Curvilinear Overset Grid Solver*

- Spalart-Allmaras turbulence model (baseline turbulence model)

## *Low-Dissipation Finite Difference Method* ([Housman et al. AIAA-2016-2963](#))

- 6th-order Hybrid Weighted Compact Nonlinear Scheme (HWCNS)
- Numerical flux is a modified Roe scheme
- 6<sup>th</sup>/5<sup>th</sup>-order blended central/upwind biased left and right state interpolation
- 2<sup>nd</sup>-order accurate differencing used for time discretization

## *Hybrid RANS/LES Models*

- Delayed Detached Eddy Simulation (DDES) model with modified length scale ([Housman et al. AIAA-2017-0640](#))
- Zonal RANS-NLES (numerical LES) with user selected zones of URANS, NLES, and wall-distance based hybrid RANS-NLES ([see paper for details](#))

## *Synthetic Eddy Method*

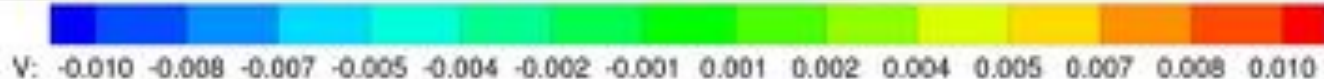
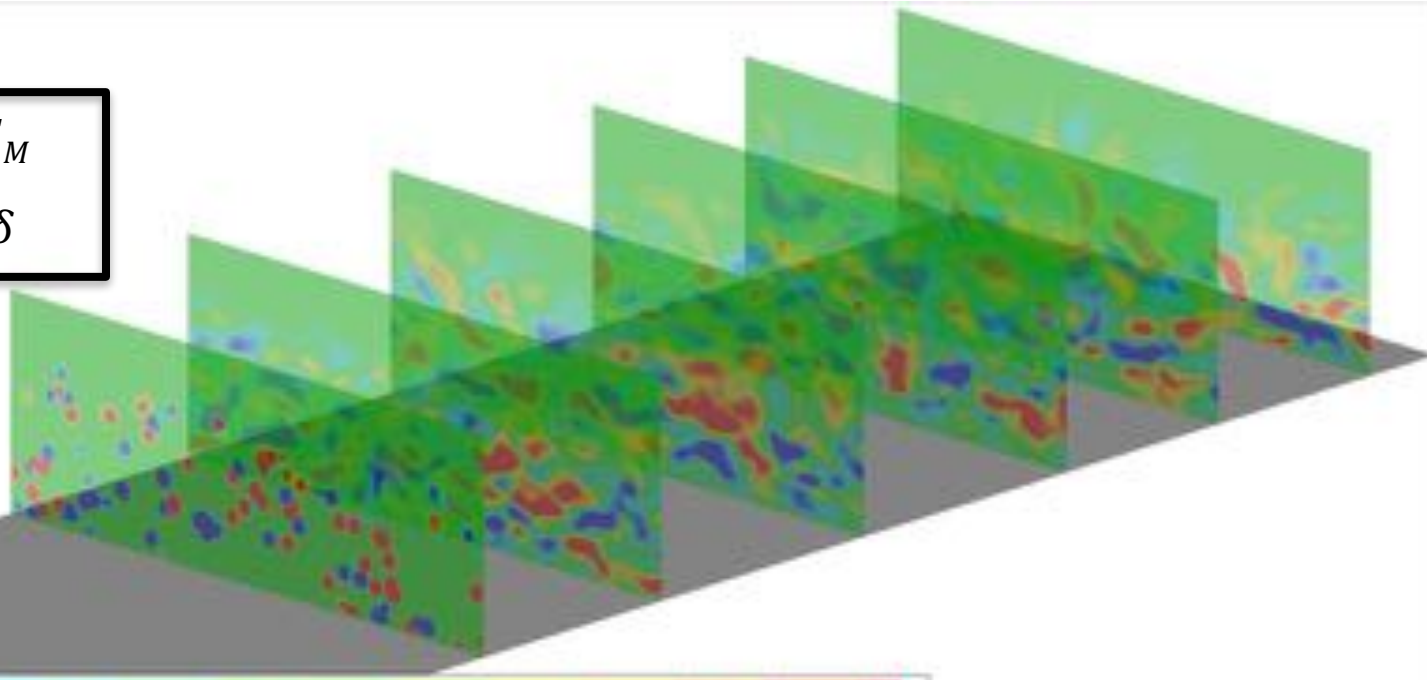
- *Coupling Methodology between RANS and LES to introduce realistic turbulent eddies* ([Jarrin et al. Int. Journal of Heat and Fluid Flow 30](#))

- When transitioning from RANS to LES in wall-bounded flows it is necessary to insert meaningful three-dimensional content at the interface
- The synthetic eddy method (SEM) is one approach which adds eddies such that first and second order turbulent statistics can be recovered. (approx. from the RANS solution with Bradshaw hypothesis)

## Jet Case SP 7

$$\Delta x S_{EM} = x e_{xit} - x S E_M$$

$$54 \delta < \Delta x S E_M < 55 \delta$$



# Computational Methodology



uRANS

$\Delta t = 1 \cdot 10^{-4}$  [s] ; 0.4 [s]



initialize Hybrid  
RANS/LES

$\Delta t = 1 \cdot 10^{-6}$  [s] ;  
time steps > 30000



final Hybrid  
RANS/LES

$\Delta t = 1 \cdot 10^{-6}$  [s]  
 $St_{\max} = 16.25$  ,  $St_{\min} = 0.008$   
 $T_{conv} \approx 205$

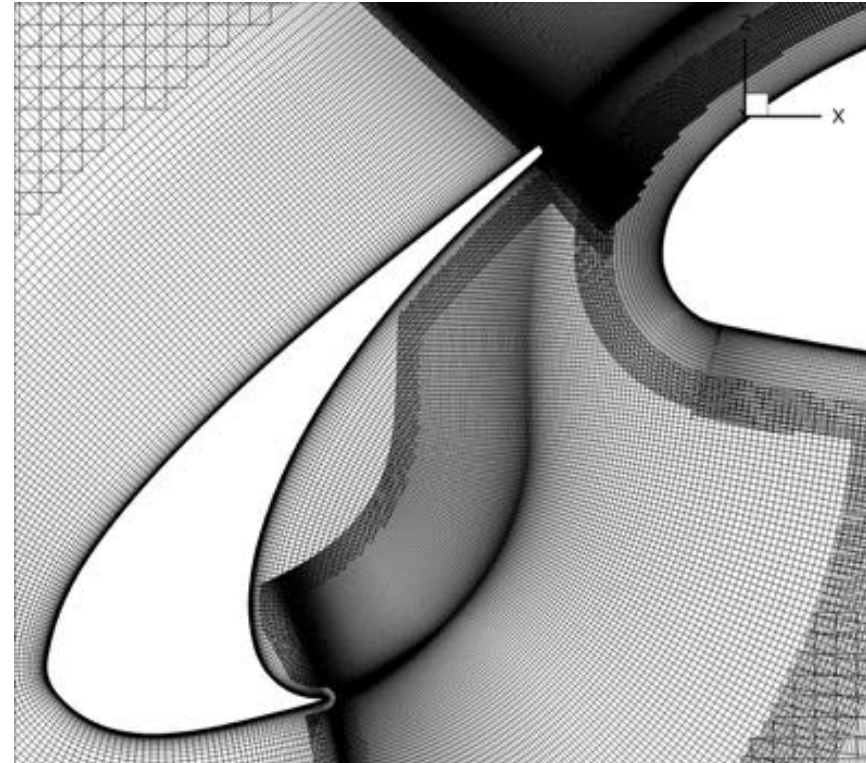
- Unsteady RANS until jet is fully developed and eddy viscosity maximum has plateaued
- Restart simulation with Hybrid RANS/LES Models until transient behavior washed out
- Ignore transients which are taken at first 30000 time steps and restart simulation
- Record Volume data at 100 kHz sampling frequency for greater than 0.02 seconds (approx. 205 convective time units)

	baseline	coarse	refined
Processors	1392 (has)	260 (ivy)	960 (has)
Wall-Clock Time [days]	12.5		
Sub-iterations	5		
Convergence	2-4 orders every sub-iteration		
Number Eddies (SEM)	-	5000	5000

# Outline

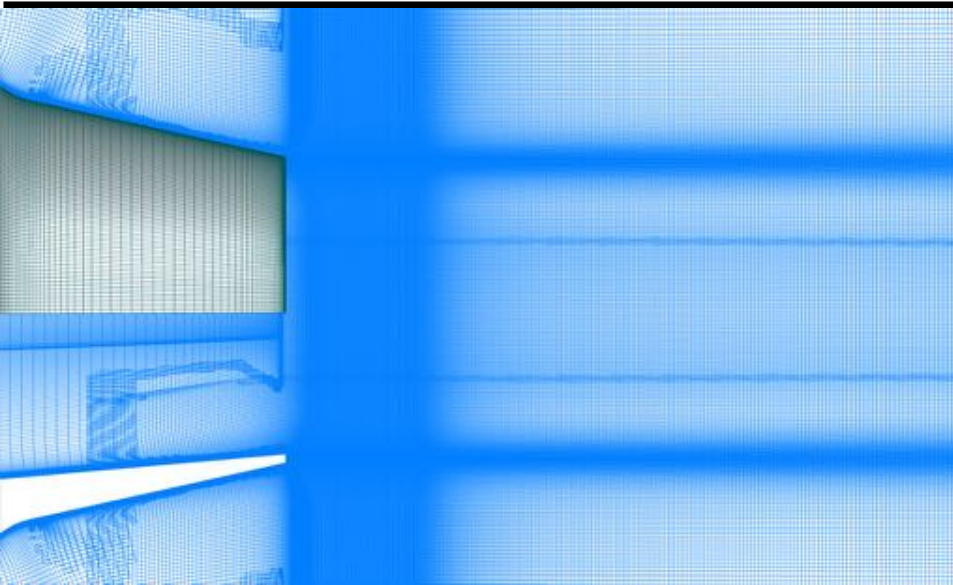


- Introduction
- Experimental Setup
- Computational Methodology
- **Structured Overset Grid System**
- Computational Results
  - Near-Field Comparison
  - Far-Field Comparison
- Summary
- Future Work



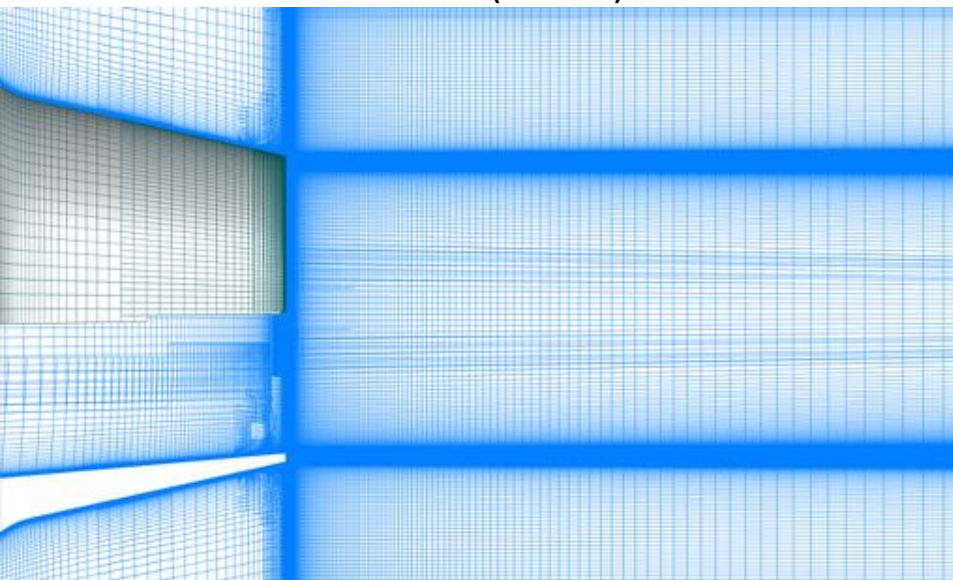


# Structured Overset Grid System

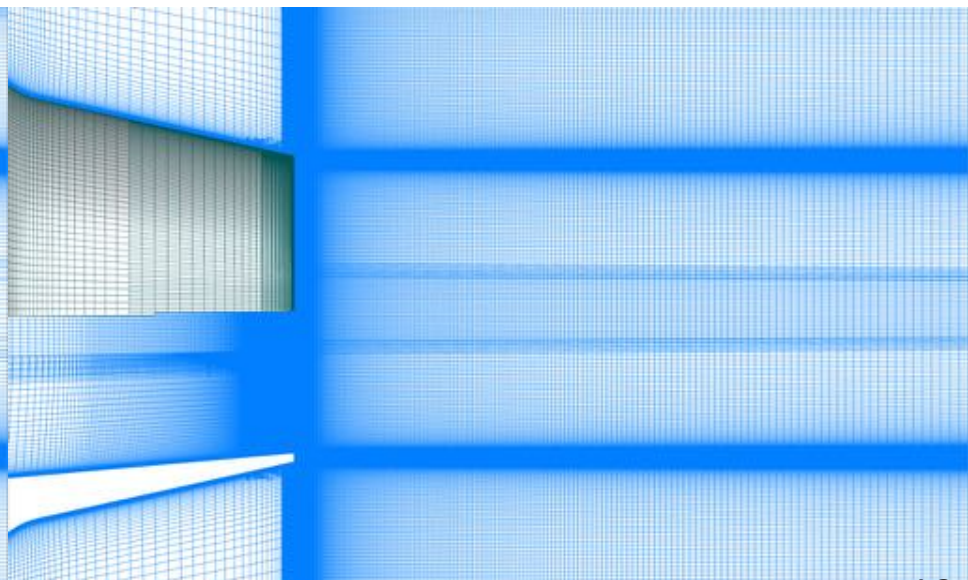


Baseline (256 M)

- Baseline (256 M)
- Coarse ( 28 M)
- Refined (106 M)
- Seven point overlap
- No orphan points
- Minimum stencil quality 0.9
- Baseline follows Bogey et. al (AIAA-2016-0261)



Coarse (28 M)



Refined (106 M)



# Structured Overset Grid System

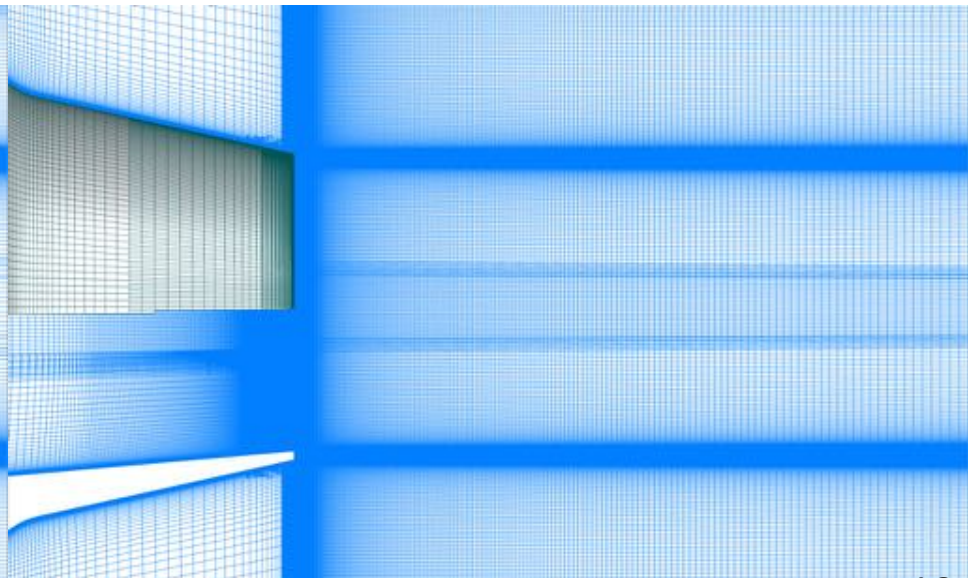


Baseline (256 M)

- Circumferential refinement in axial and radial direction  
Bres *et. al.* (AIAA-2015-2535)



Coarse (28 M)



Refined (106 M)

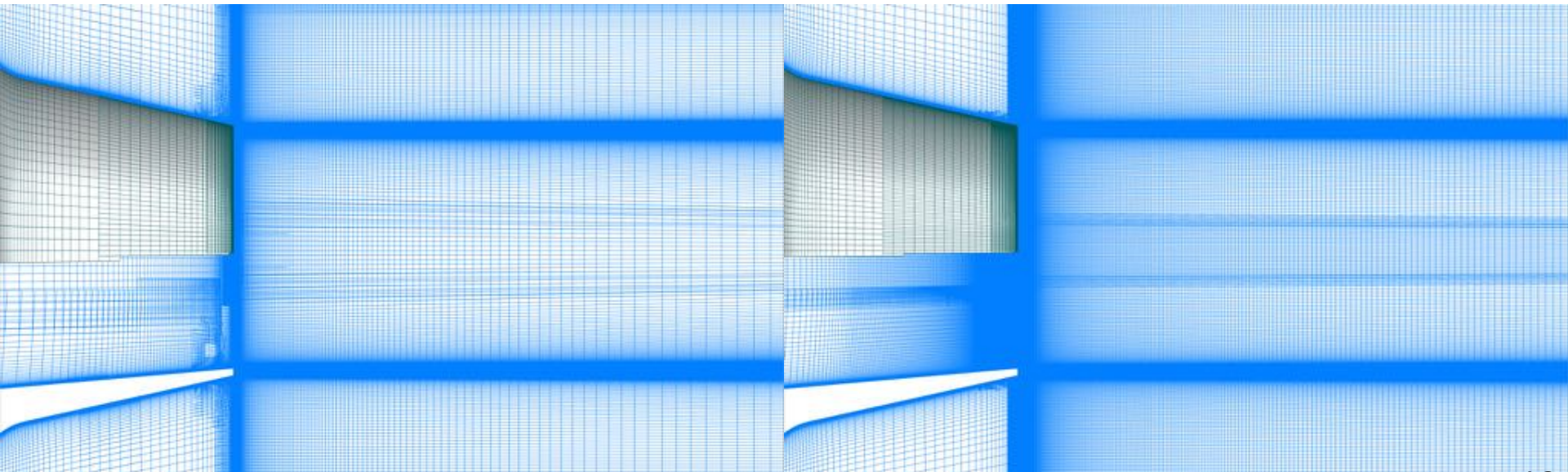
# Structured Overset Grid System



circumferential  
refinement



- Circumferential refinement in axial and radial direction  
Bres *et. al.* (AIAA-2015-2535)

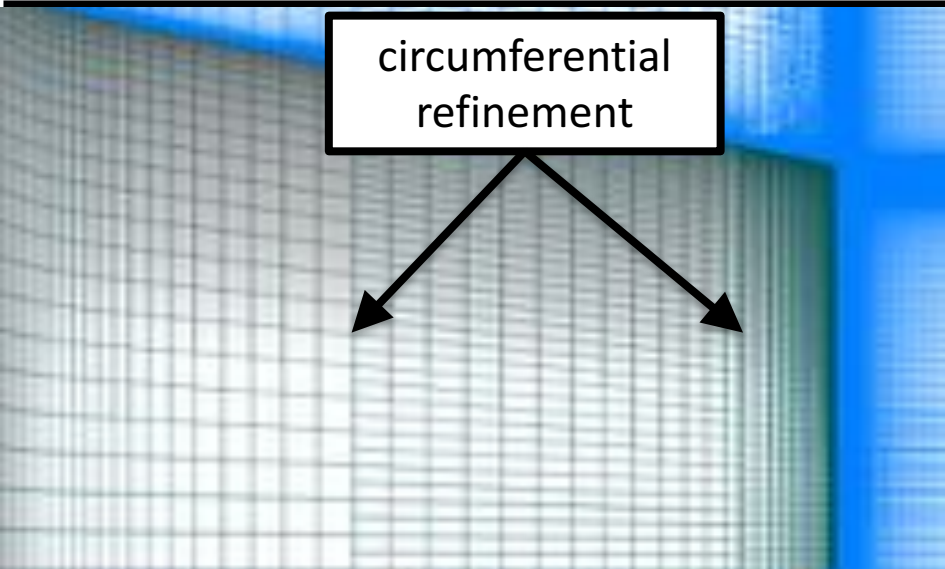


Coarse (28 M)

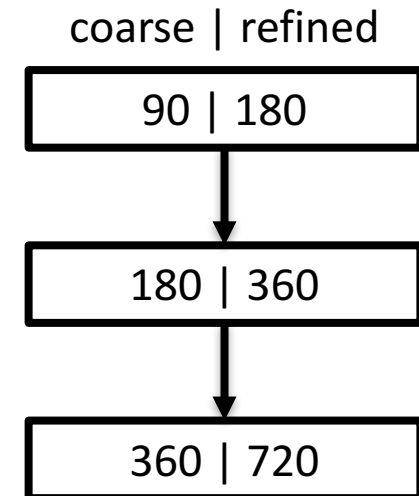
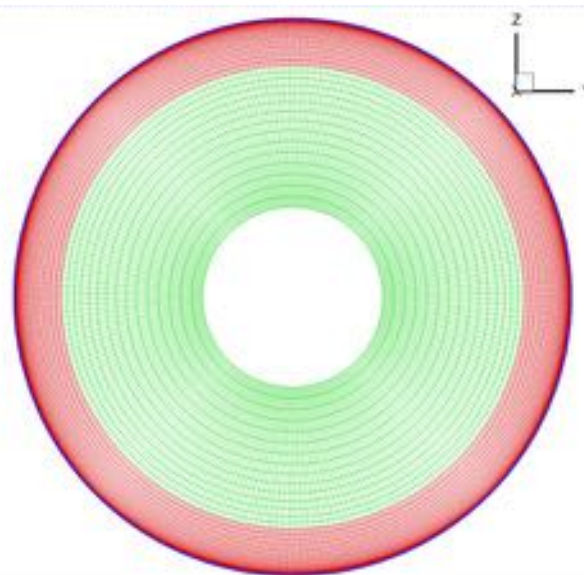
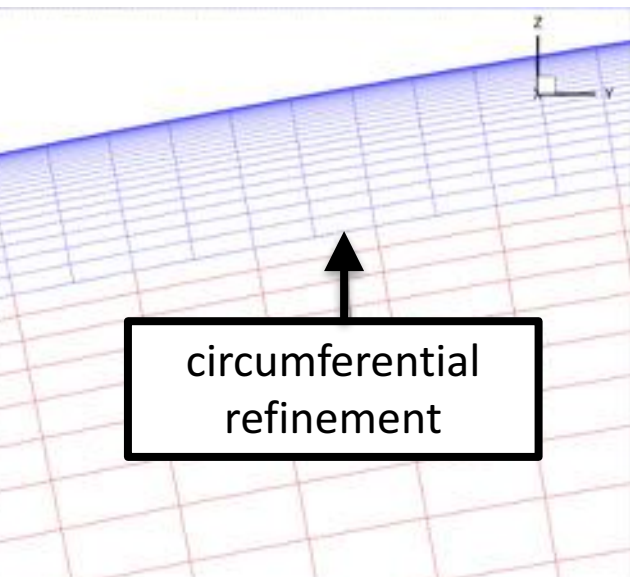
Refined (106 M)



# Structured Overset Grid System

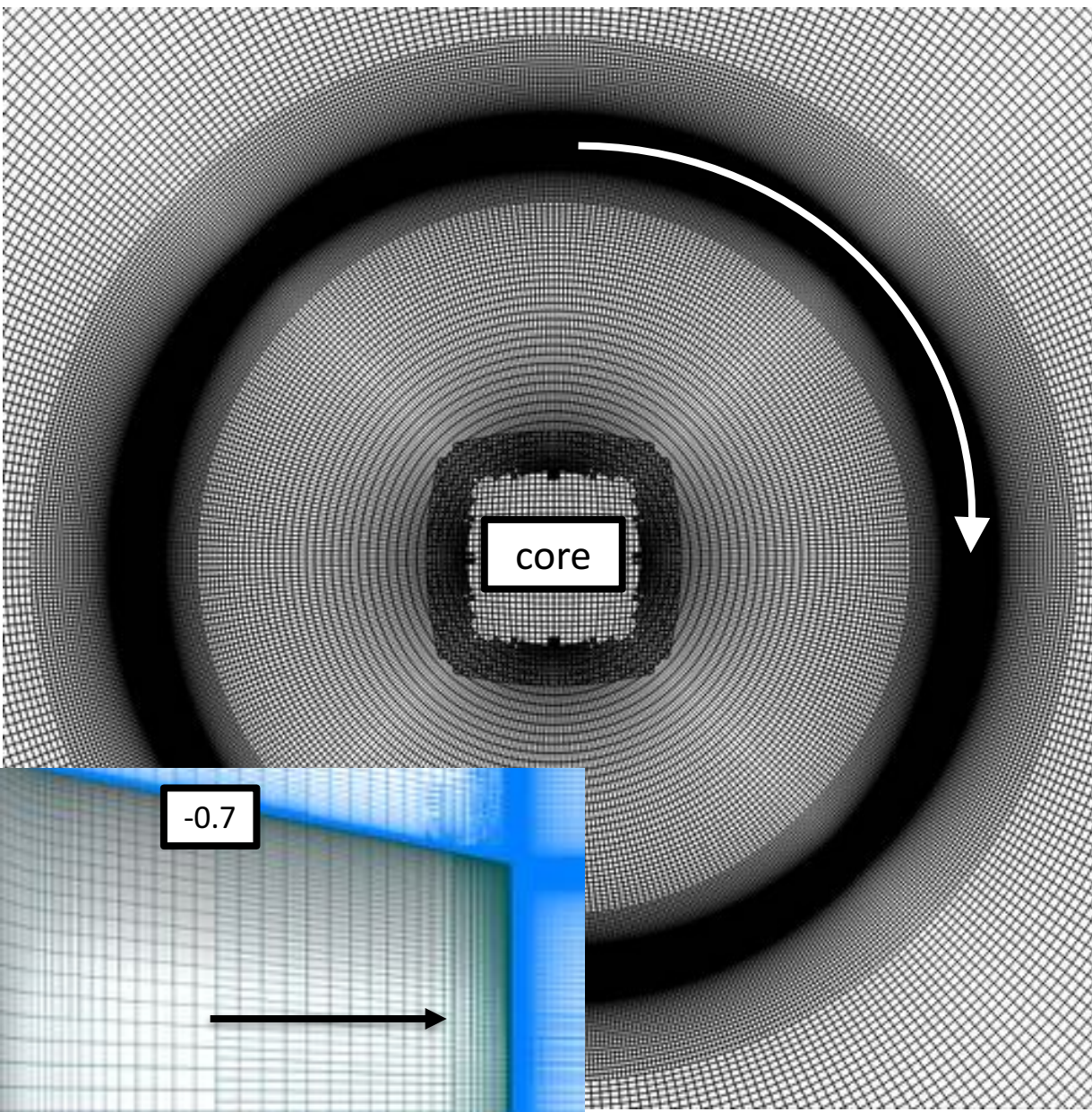


- Circumferential refinement in axial and radial direction  
Bres *et. al.* (AIAA-2015-2535)



baseline 360

# Structured Overset Grid System



## axial/radial AR

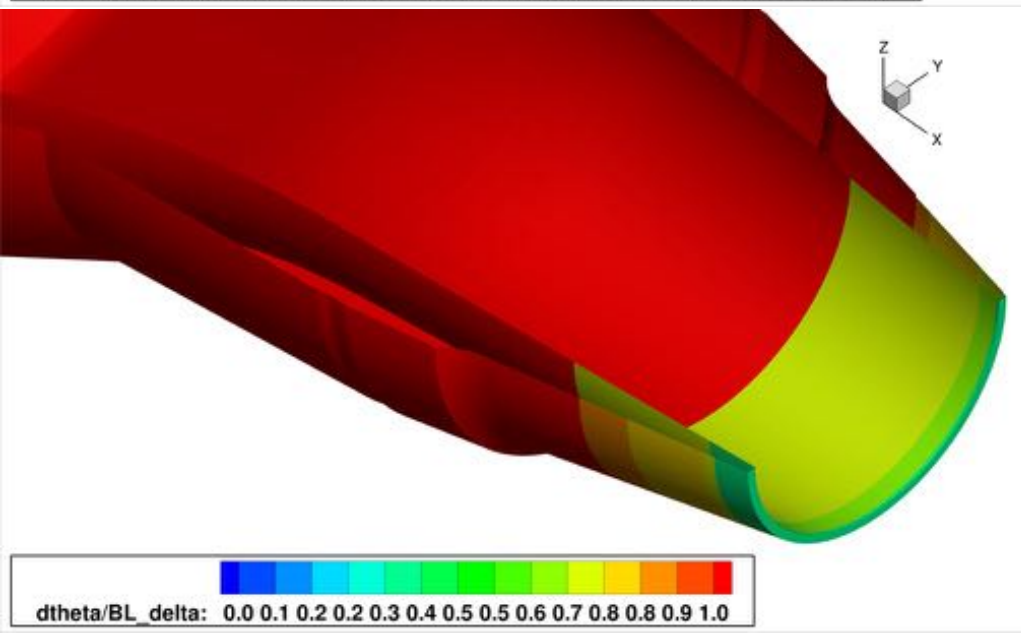
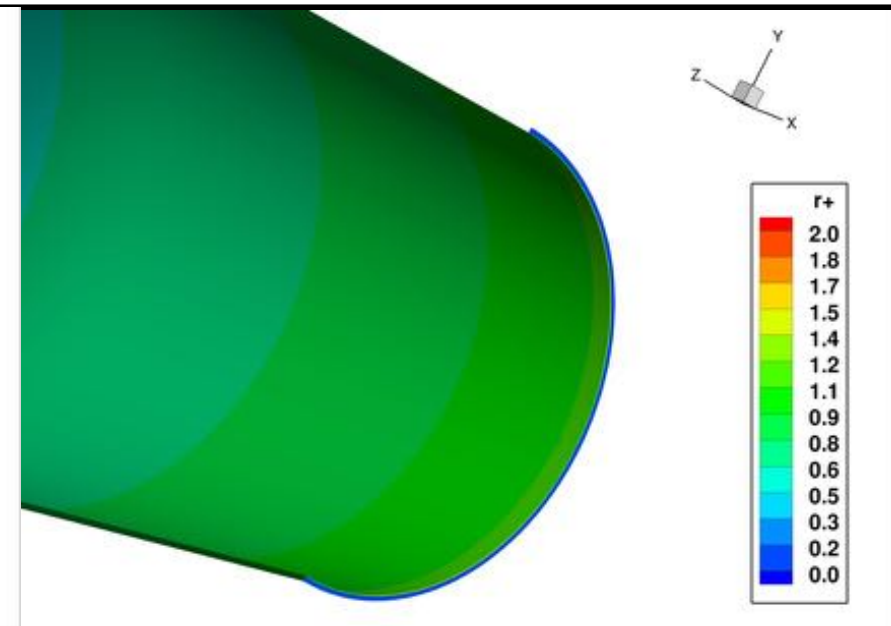
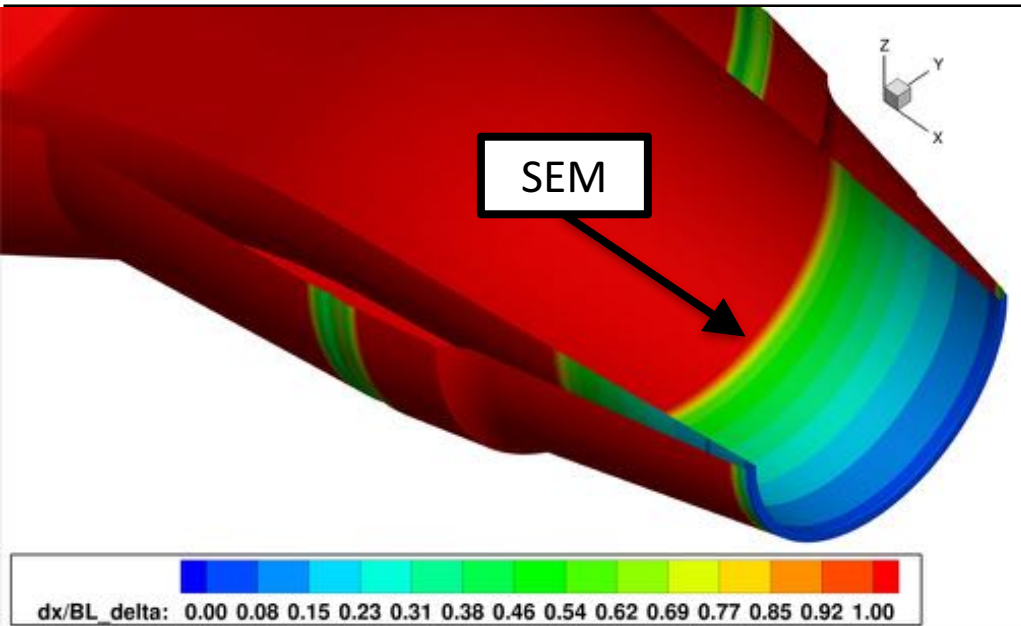
	$(x-x_{\text{exit}})/D$	AR
wall	-0.7	321.15
core	-0.7	0.50
wall	0.0	34.50
core	0.0	0.06
shear	0.5 – 25.0	10.50
core	0.5 – 25.0	1.05

## circumferential/radial AR

	$(x-x_{\text{exit}})/D$	AR
wall	-0.7	436.82
core	-0.7	1.00
wall	0.0	221.00
core	0.0	1.00
shear	0.5 – 25.0	1134
core	0.5 – 25.0	1.00



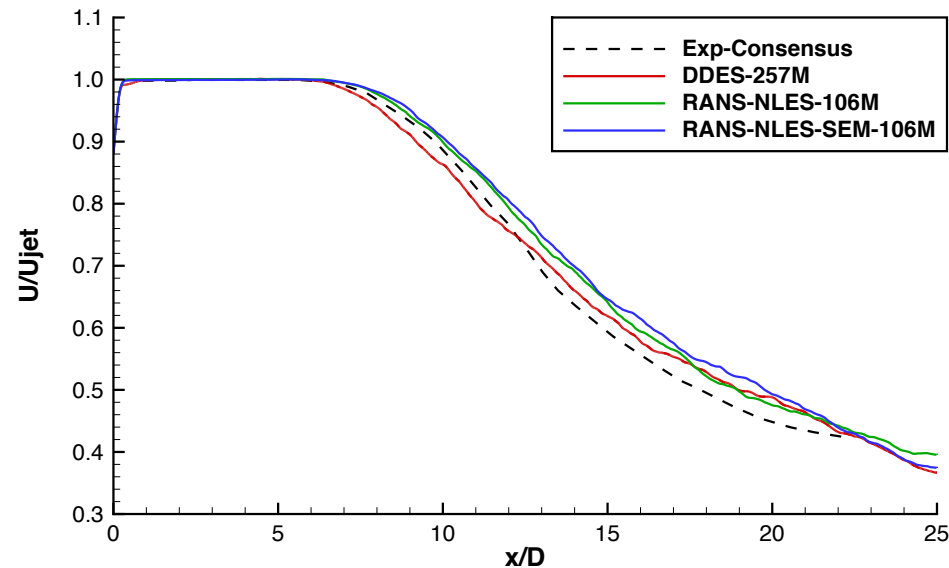
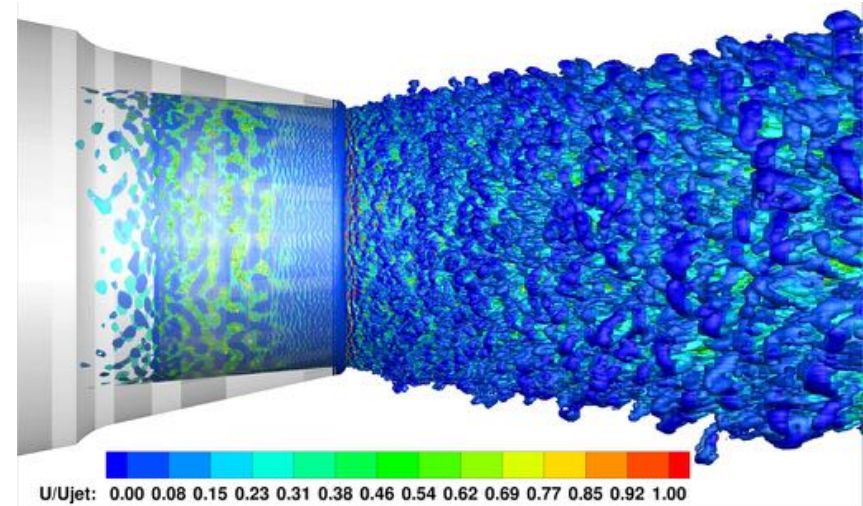
# Structured Overset Grid System



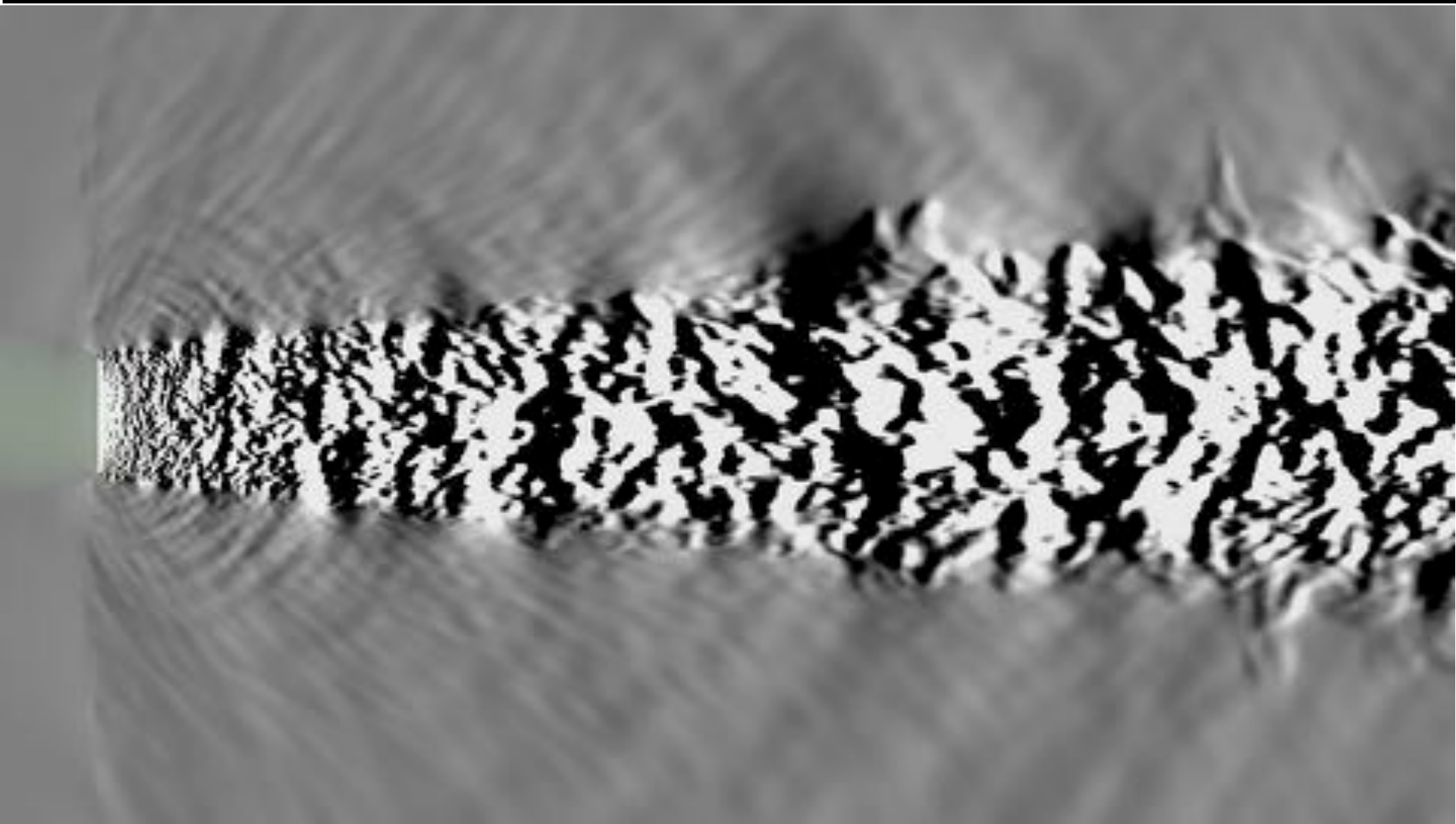
# Outline



- Introduction
- Experimental Setup
- Computational Methodology
- Structured Overset Grid System
- **Computational Results**
  - Near-Field Comparison
  - Far-Field Comparison
- Summary
- Future Work



# Computational Results

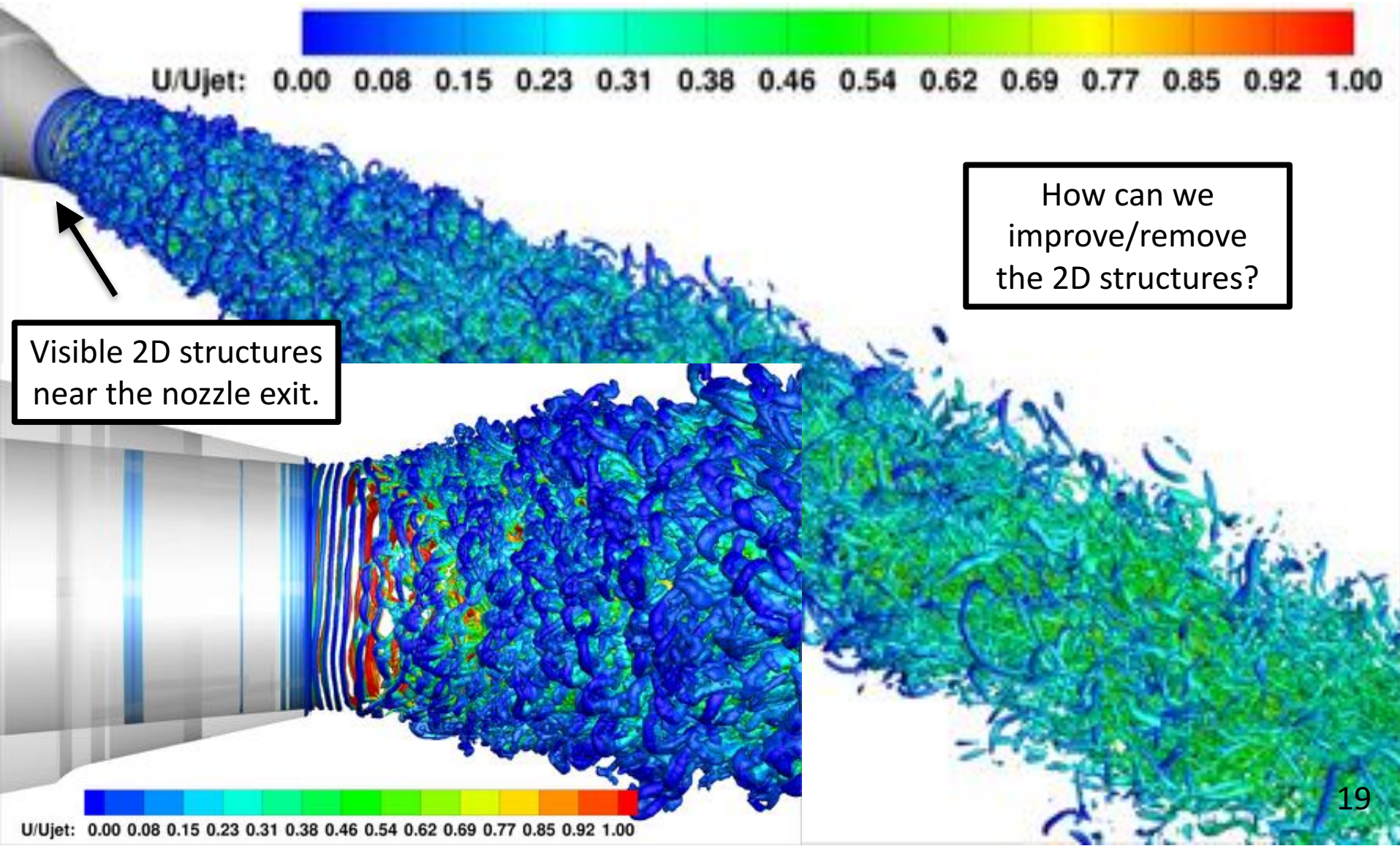




# Computational Results



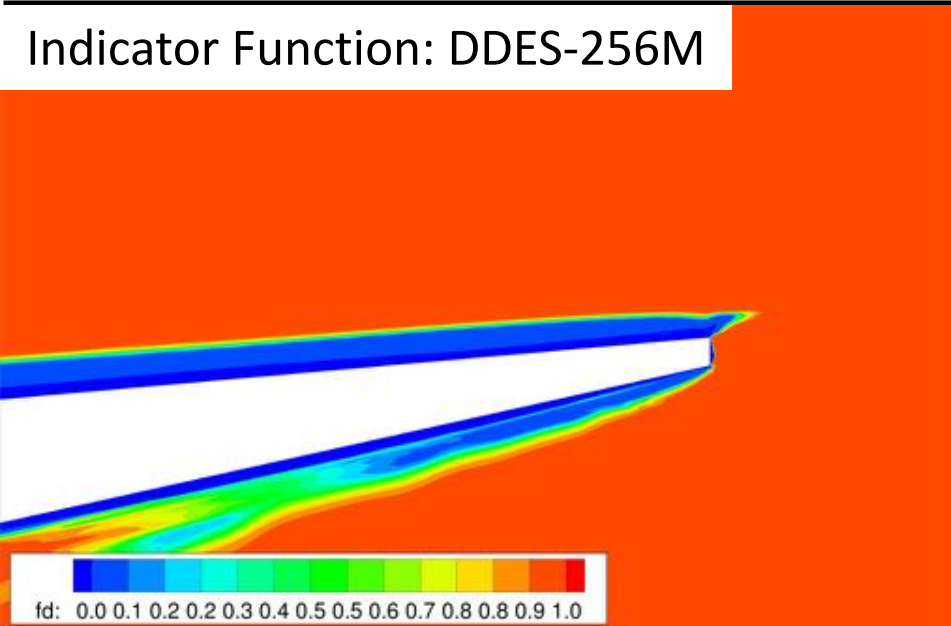
Flow Field Visualization: Iso-contours of Q-criteria colored by axial velocity



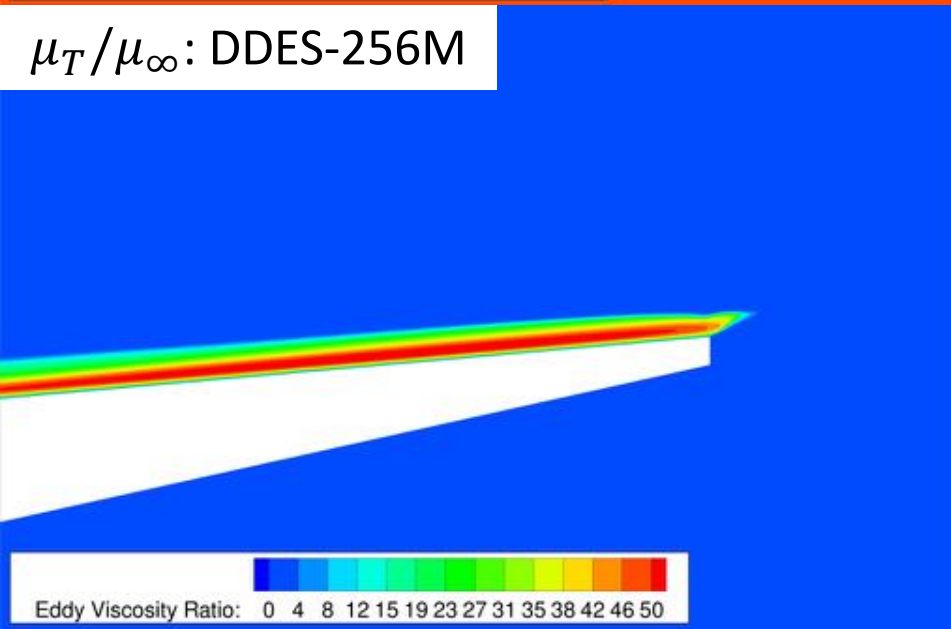
# Computational Results



Indicator Function: DDES-256M



$\mu_T/\mu_\infty$ : DDES-256M



- Indicator function  $f_d$  indicates RANS or LES mode.
- Stays in RANS mode in nozzle interior and quickly transitions to LES downstream of nozzle lip
- Retains large eddy viscosity throughout the boundary layer

- Shielding function RANS-NLES:

$$f_d = 1 - \frac{1}{2} \left[ 1 - \tanh(\epsilon_d(d_{wall} - d_0)) \right]$$

$d_{wall}$  : walldistance

$d_0$  : transition distance (user)

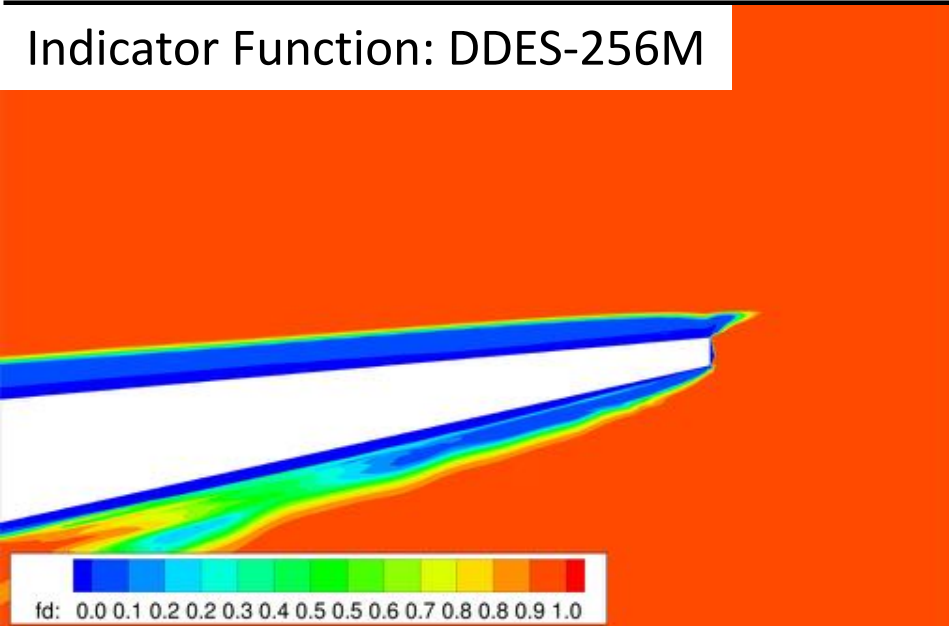
$\epsilon_d$  : blending (user)



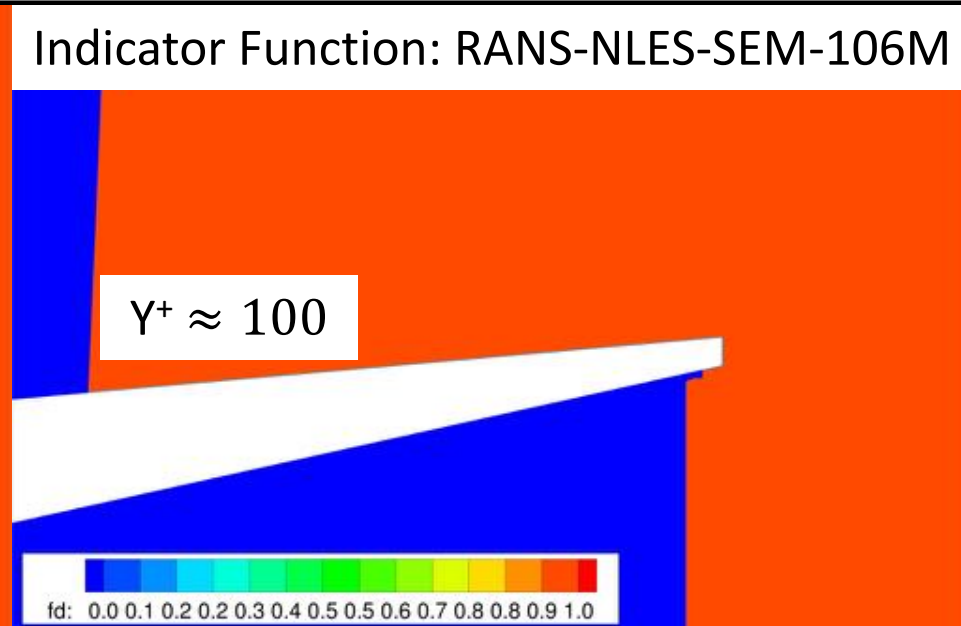
# Computational Results



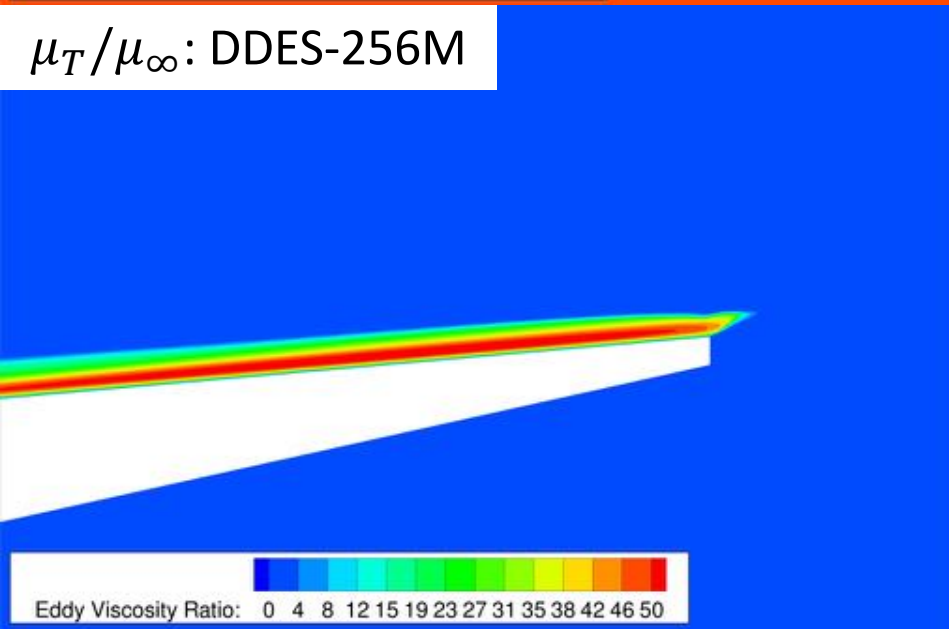
Indicator Function: DDES-256M



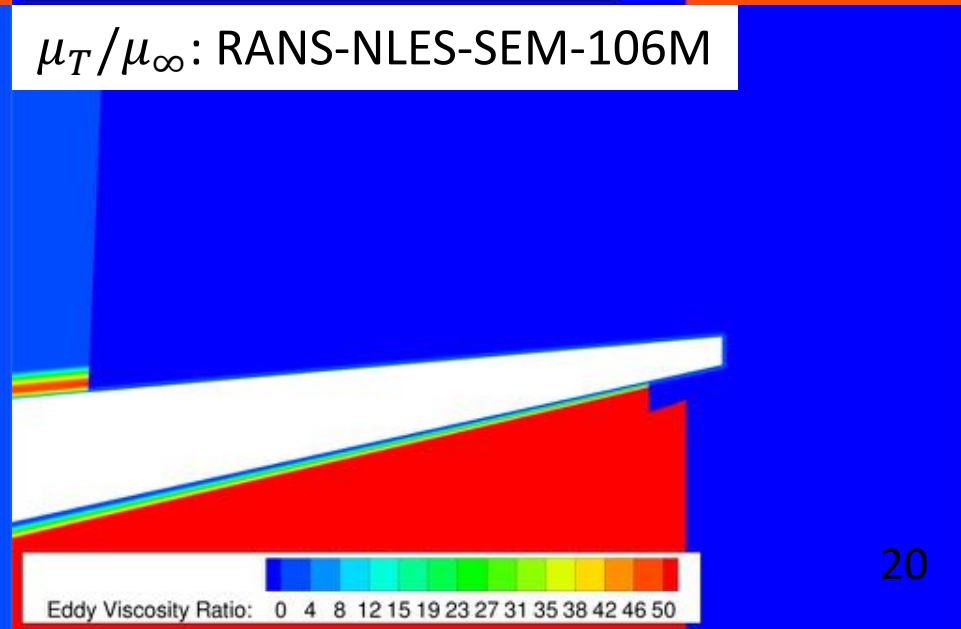
Indicator Function: RANS-NLES-SEM-106M



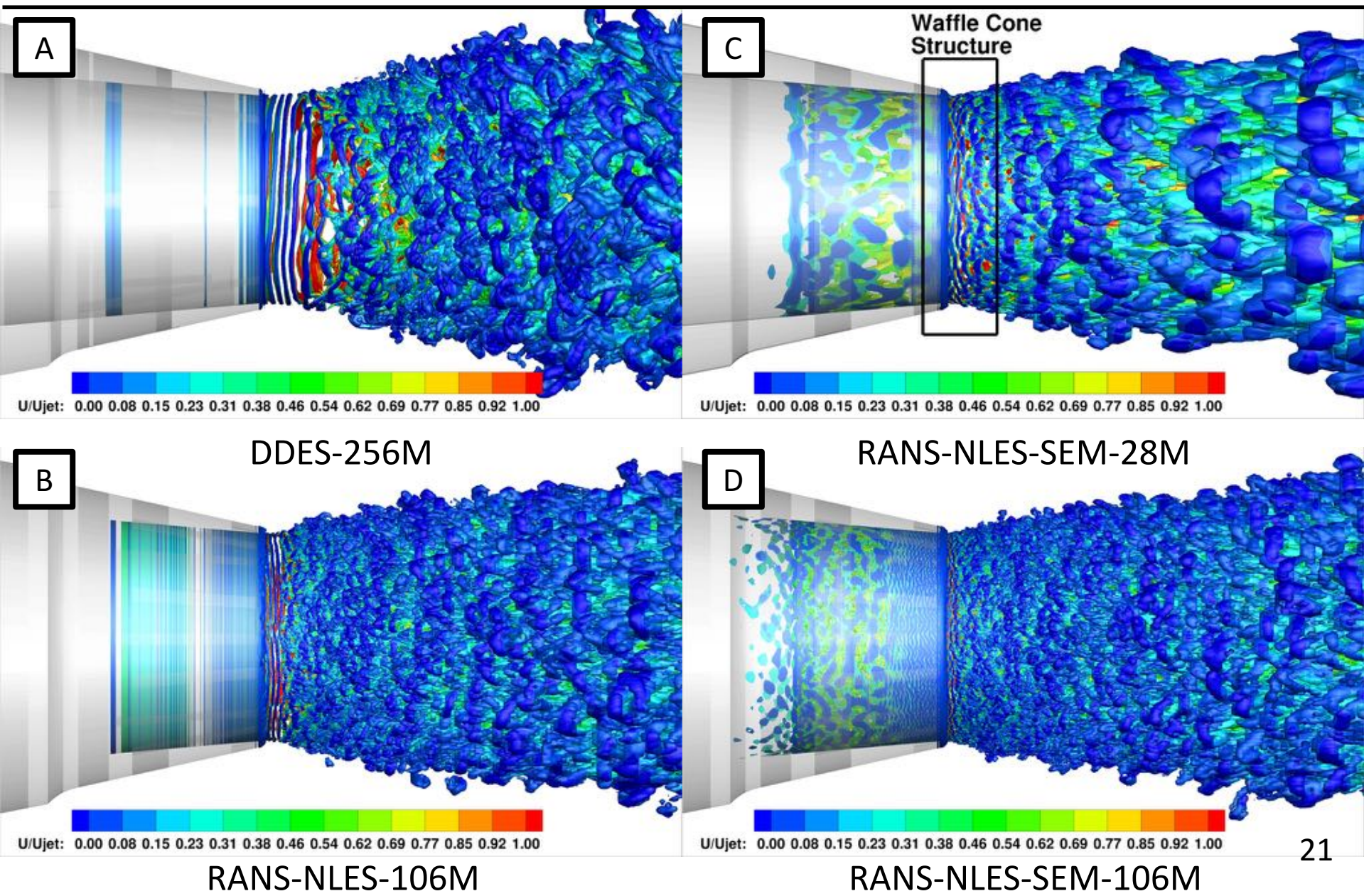
$\mu_T/\mu_\infty$ : DDES-256M



$\mu_T/\mu_\infty$ : RANS-NLES-SEM-106M



# Computational Results

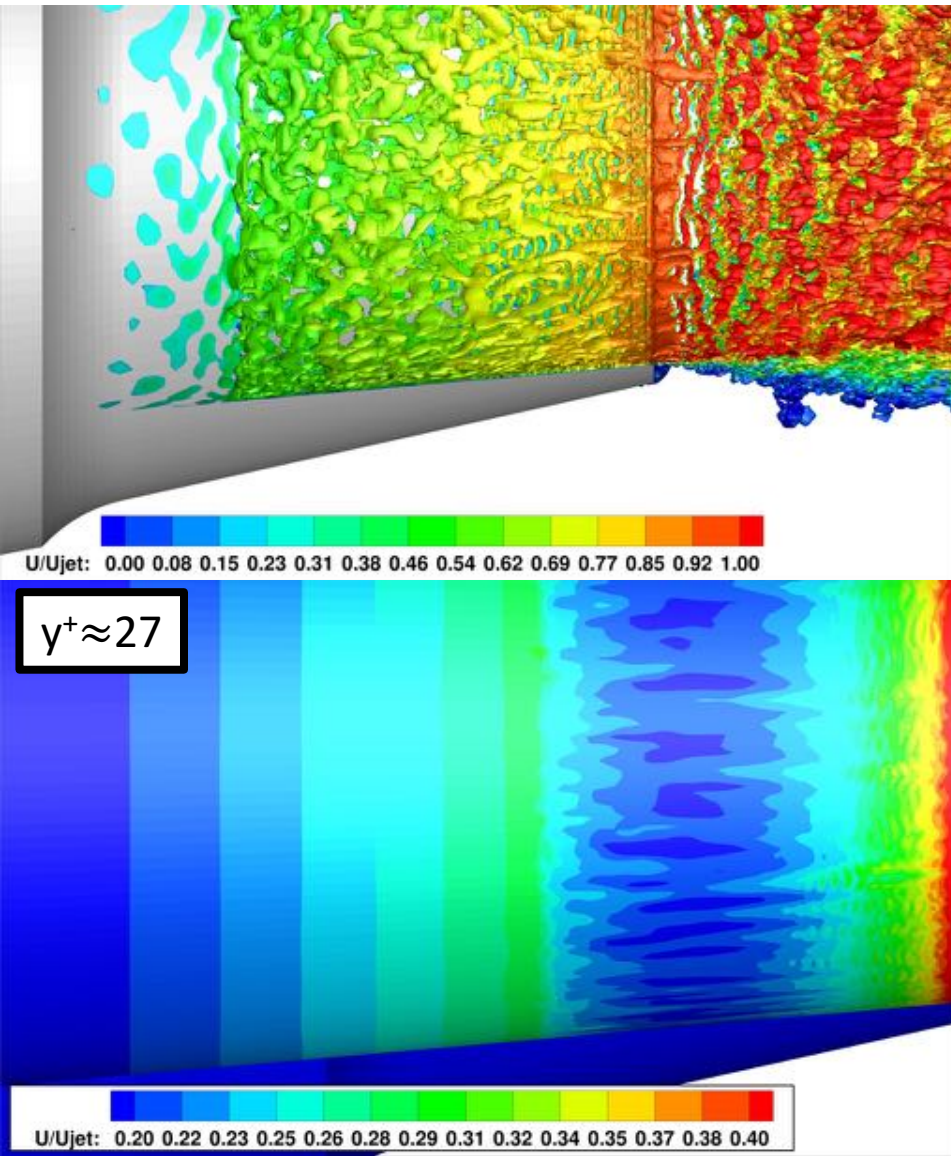




# Computational Results



## RANS-NLES-SEM Refined Mesh

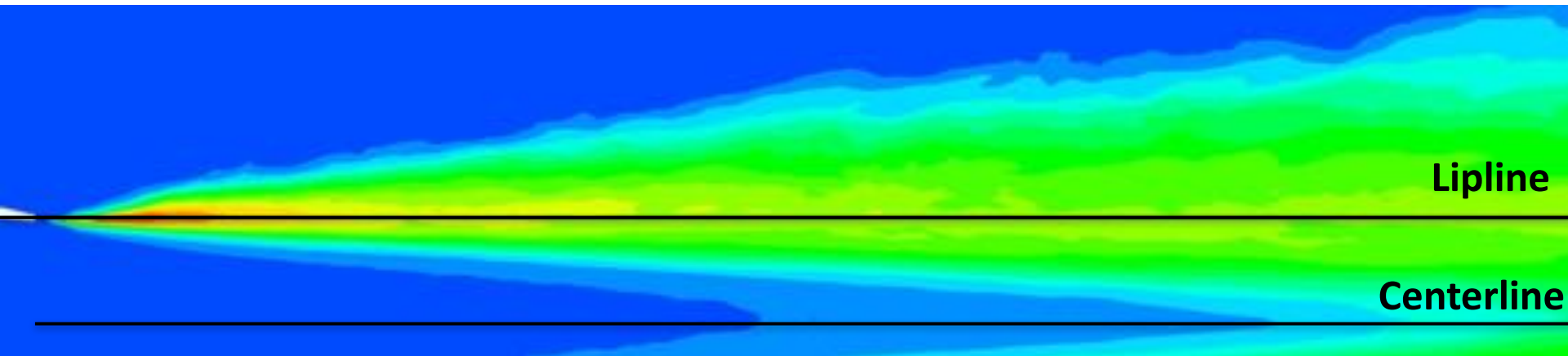


- Quasi-2D waffle cone structures at nozzle exit
- Size of turbulent structures appears to be too large inside nozzle
- Structures deep in the boundary layer show very little azimuthal variation
- Features are elongated and too highly correlated in both the streamwise and azimuthal direction
- *Do we have realistic, fully developed BL turbulence at the exit?*



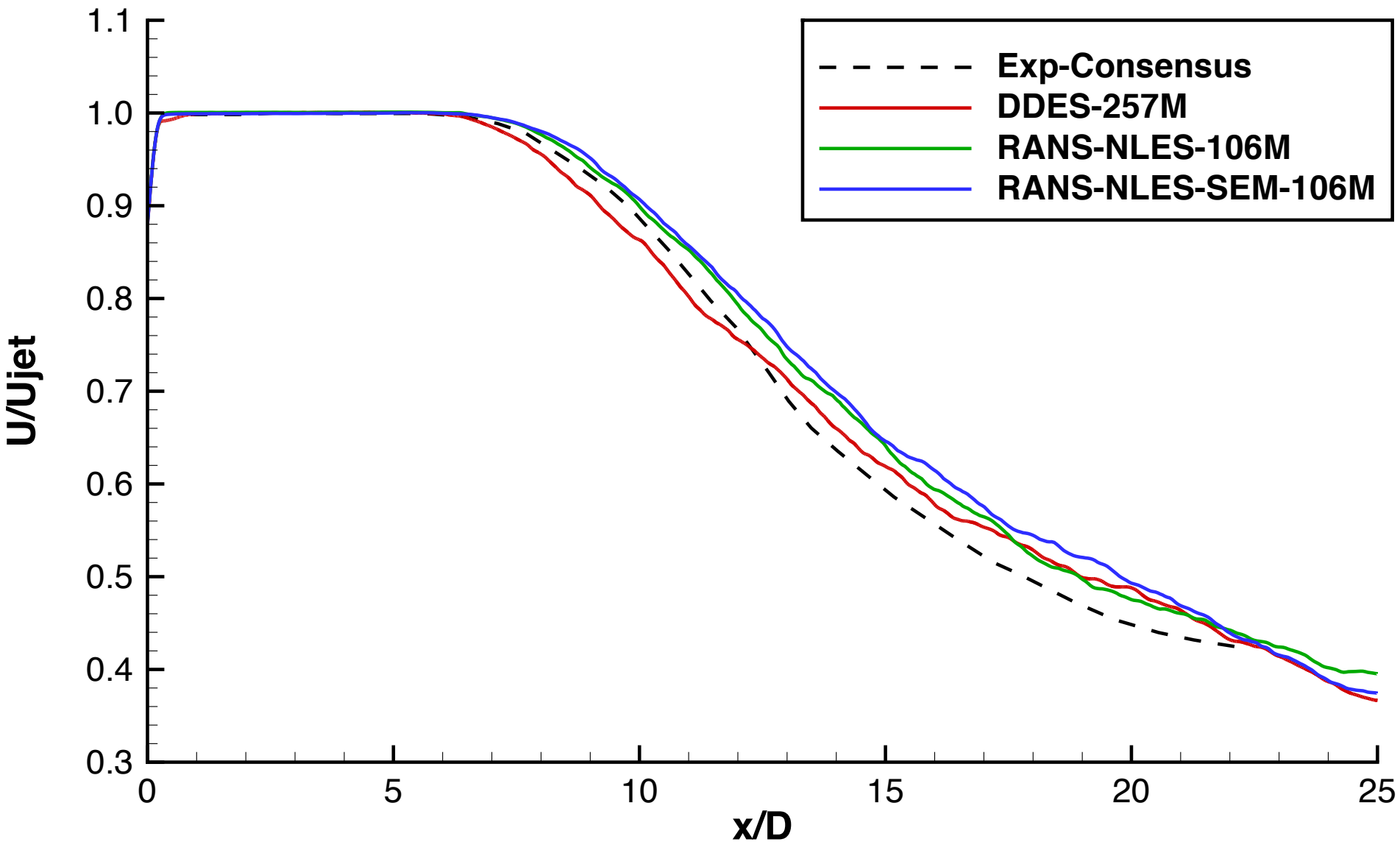
# Computational Results – Near-Field

## Near-Field Comparison

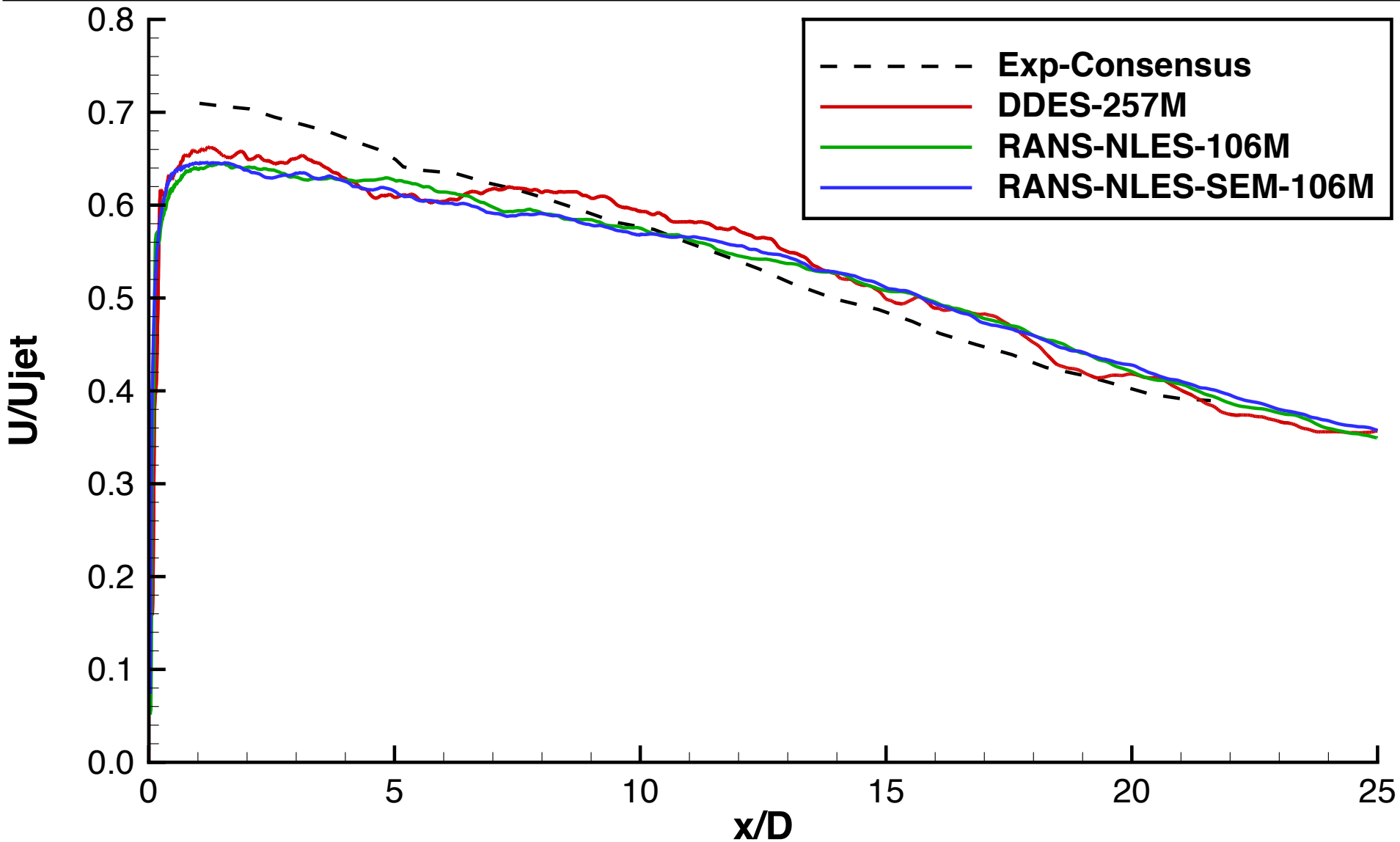


- Near field turbulent statistics computed from DDES, RANS-NLES and RANS-NLES-SEM models for comparison with PIV data from the SHJAR
- Comparison of measurements to data at lipline ( $z/R=1$ ) and centerline ( $z/R=0$ )

# Near-Field: Time-Averaged Centerline

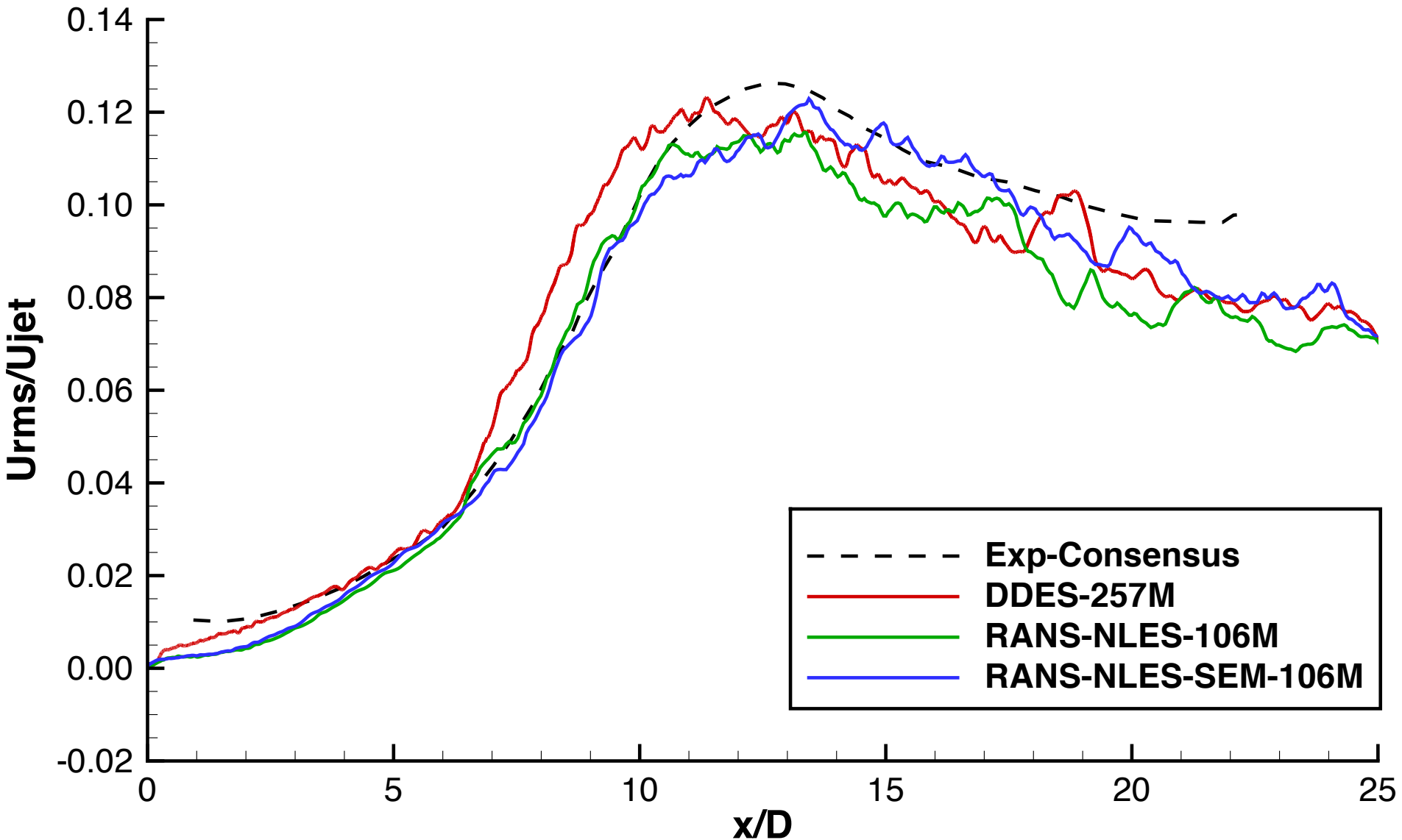


# Near-Field: Time-Averaged Lipline

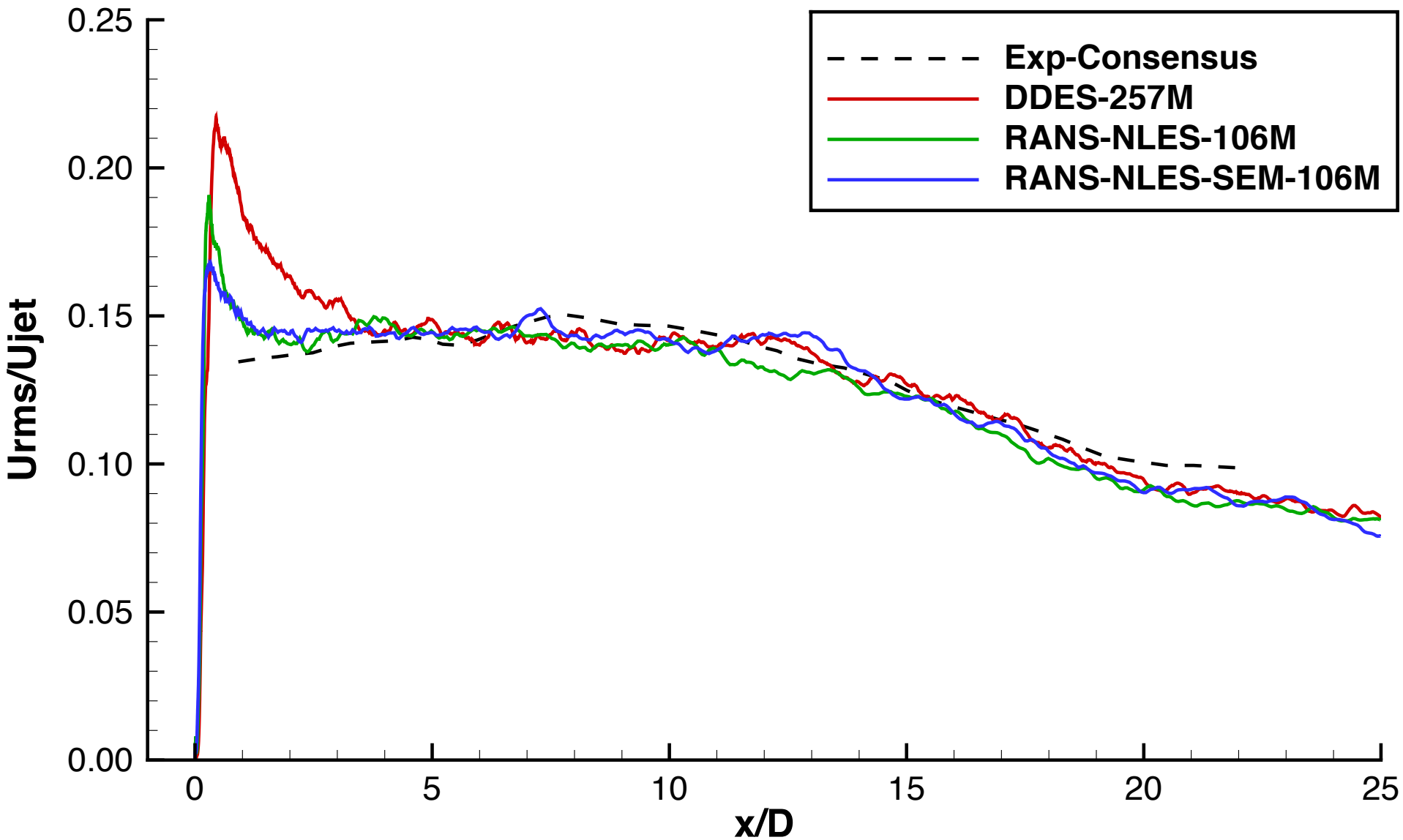




# Near-Field: RMS Centerline



# Near-Field: RMS Lipline



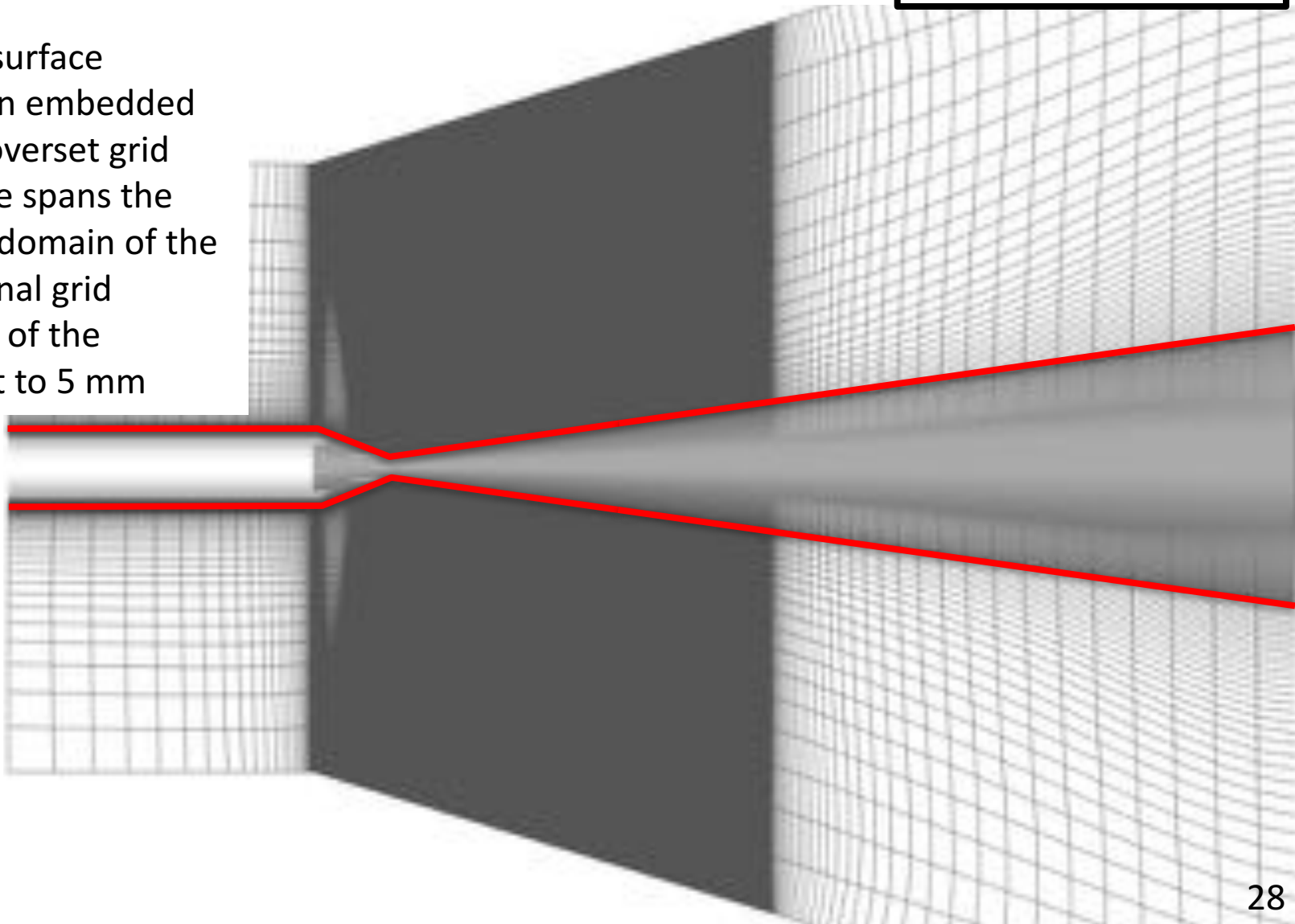
# Computational Results – Far-Field



## FWH Permeable Surface

Observers 100 D away

- Generated surface triangulation embedded within the overset grid
- FWH surface spans the entire axial domain of the computational grid
- Edge length of the triangles set to 5 mm





# Computational Results – Far-Field

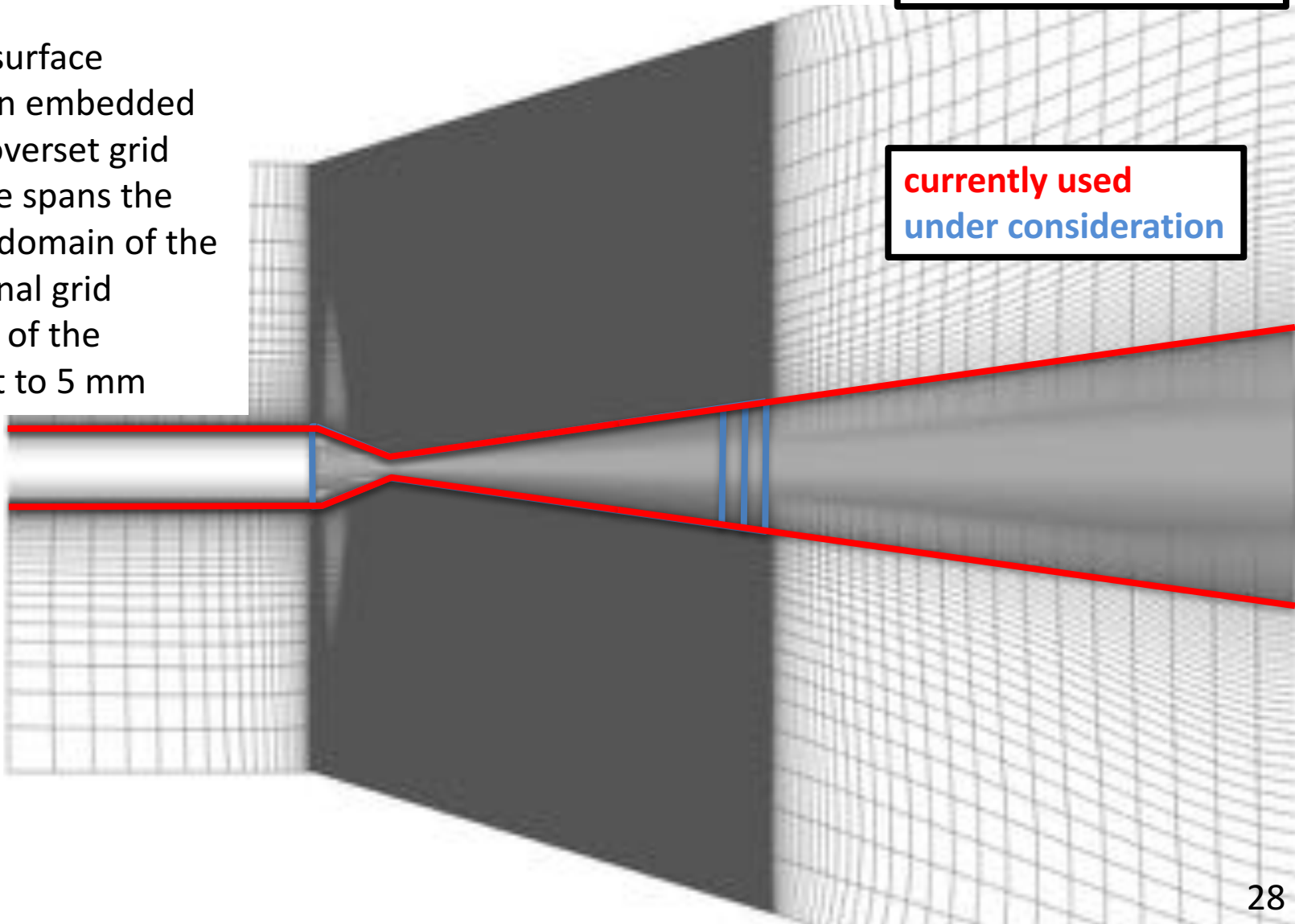


## FWH Permeable Surface

- Generated surface triangulation embedded within the overset grid
- FWH surface spans the entire axial domain of the computational grid
- Edge length of the triangles set to 5 mm

Observers 100 D away

currently used  
under consideration

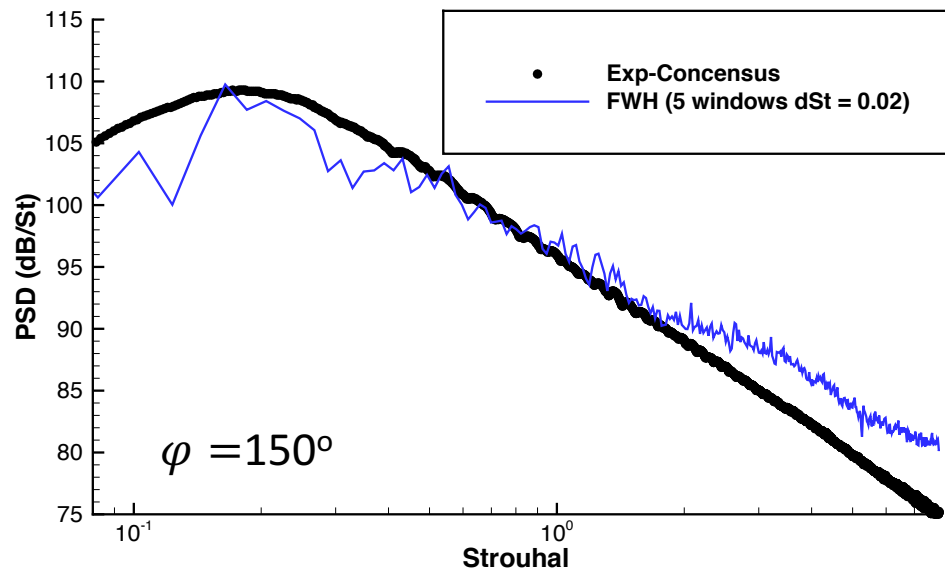
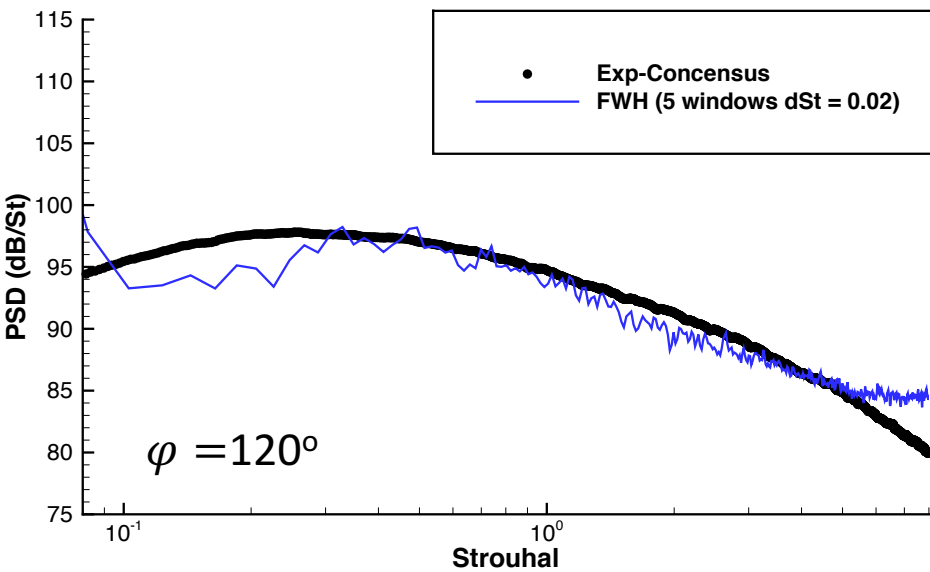
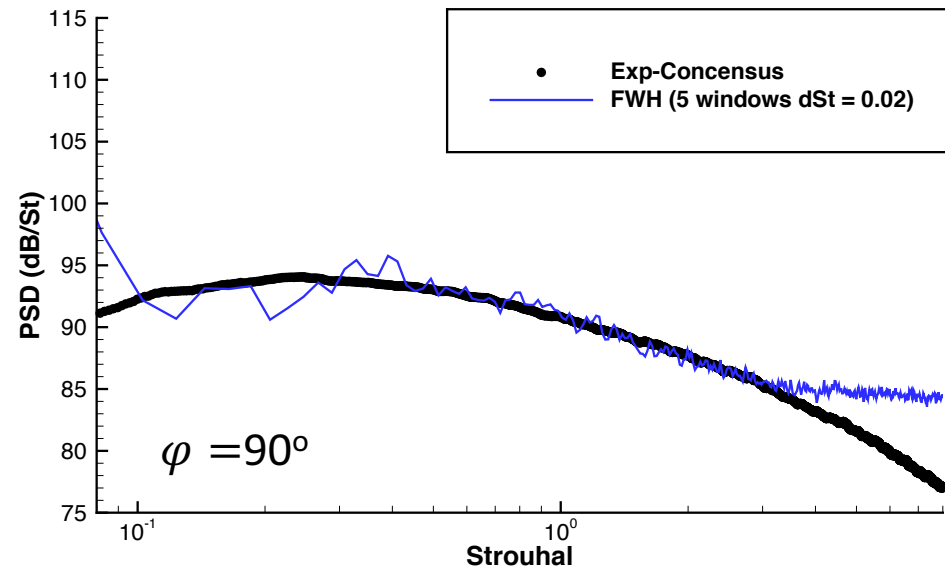
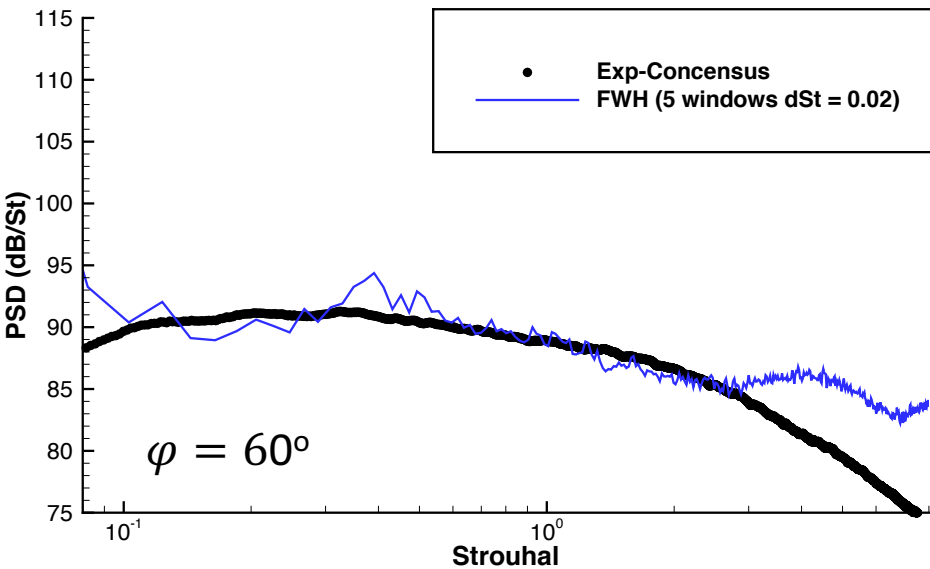


# Computational Results – Far-Field



- Interpolate Volume solution to FWH surface at sampling rate of  $\Delta t = 0.00001$  s (100 kHz)
- Split time sample into 5 windows (or segments) with 50% overlap at  $St_{bin} = 0.02$
- Compute Integrands of FWH over each window independently
  - $Q_n, F_1, F_2, F_3$
  - Hanning Window is applied in the time-domain
  - FFT is applied and stored for computing far-field observer noise levels
- FWH surface integrals computed over each observer and window
  - 360 observers, uniformly distributed along the azimuth, for each angle ( $60^\circ, 90^\circ, 120^\circ, 150^\circ$ )
  - The PSD is ensemble averaged over the 360 observers
  - PSD is multiplied by  $\sqrt{8/3}$  to recover RMS levels lost from Hanning Window
- Finally, PSD spectrum is averaged over the 5 windows for final comparison to the experimental consensus.

# Computational Results – Far-Field

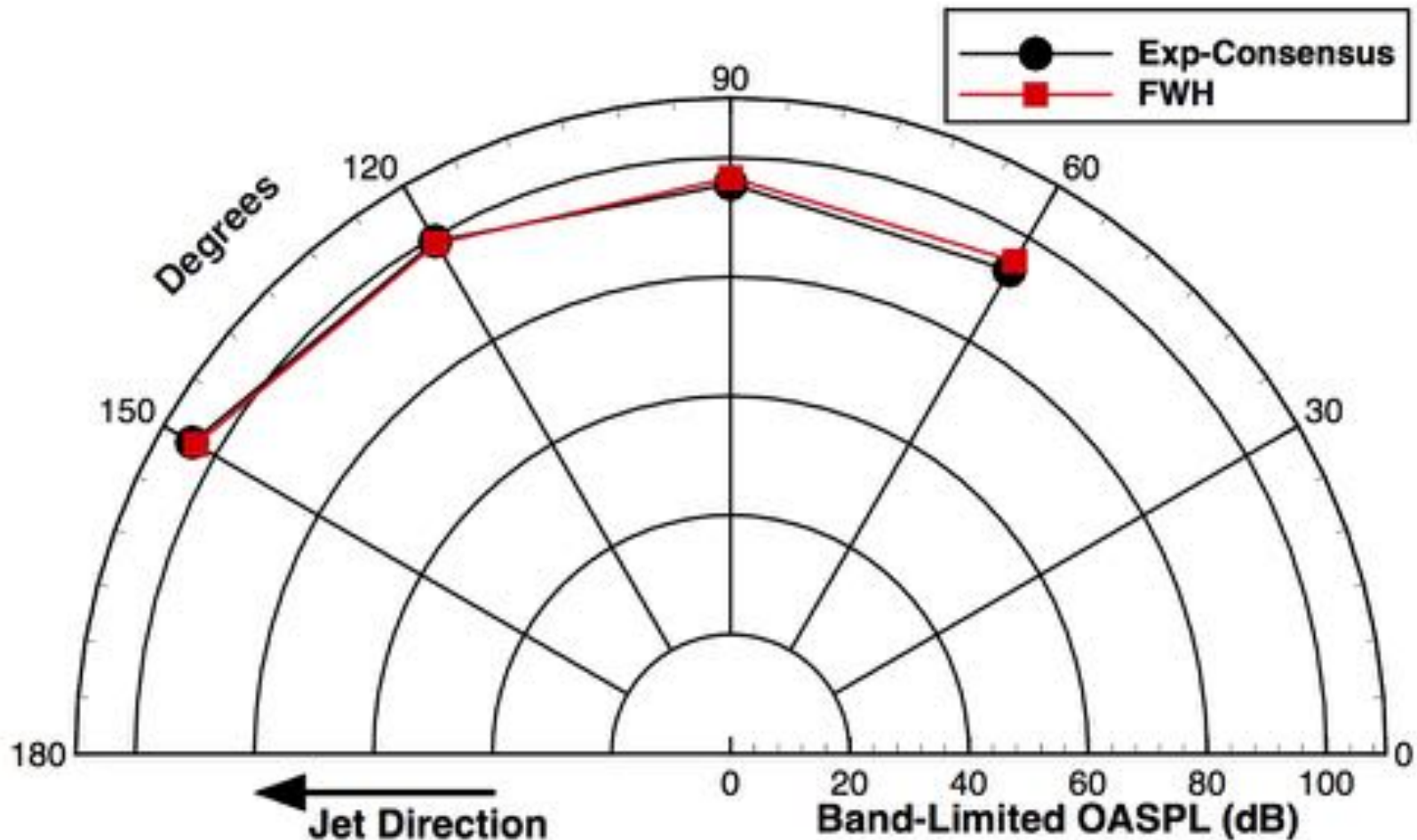


Far-Field Comparison: PSD Spectrum at 100D from exit



# Computational Results – Far-Field

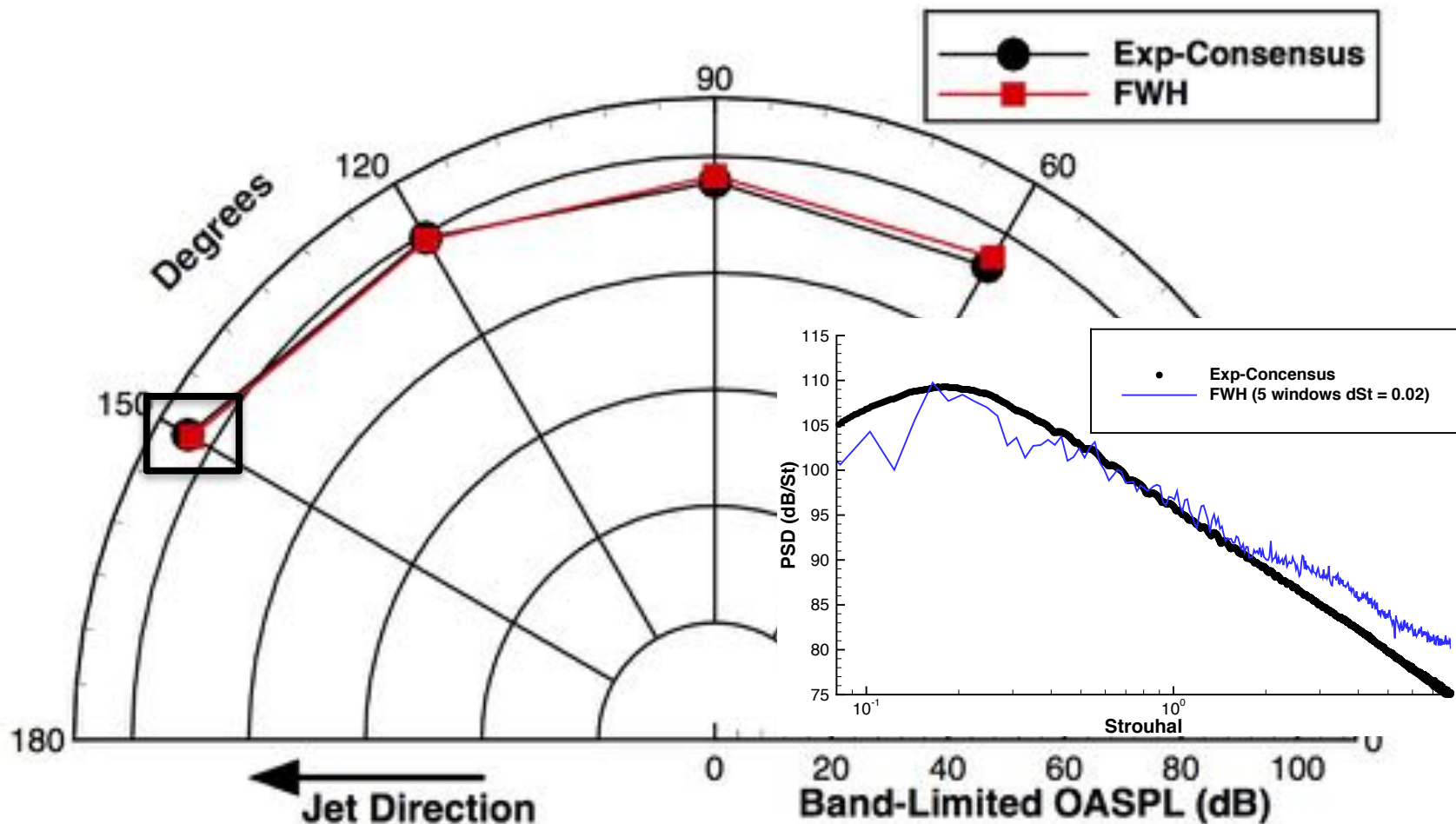
Far-Field Comparison: Band-Limited OASPL ( $0.08 \leq St \leq 8.0$ )



# Computational Results – Far-Field



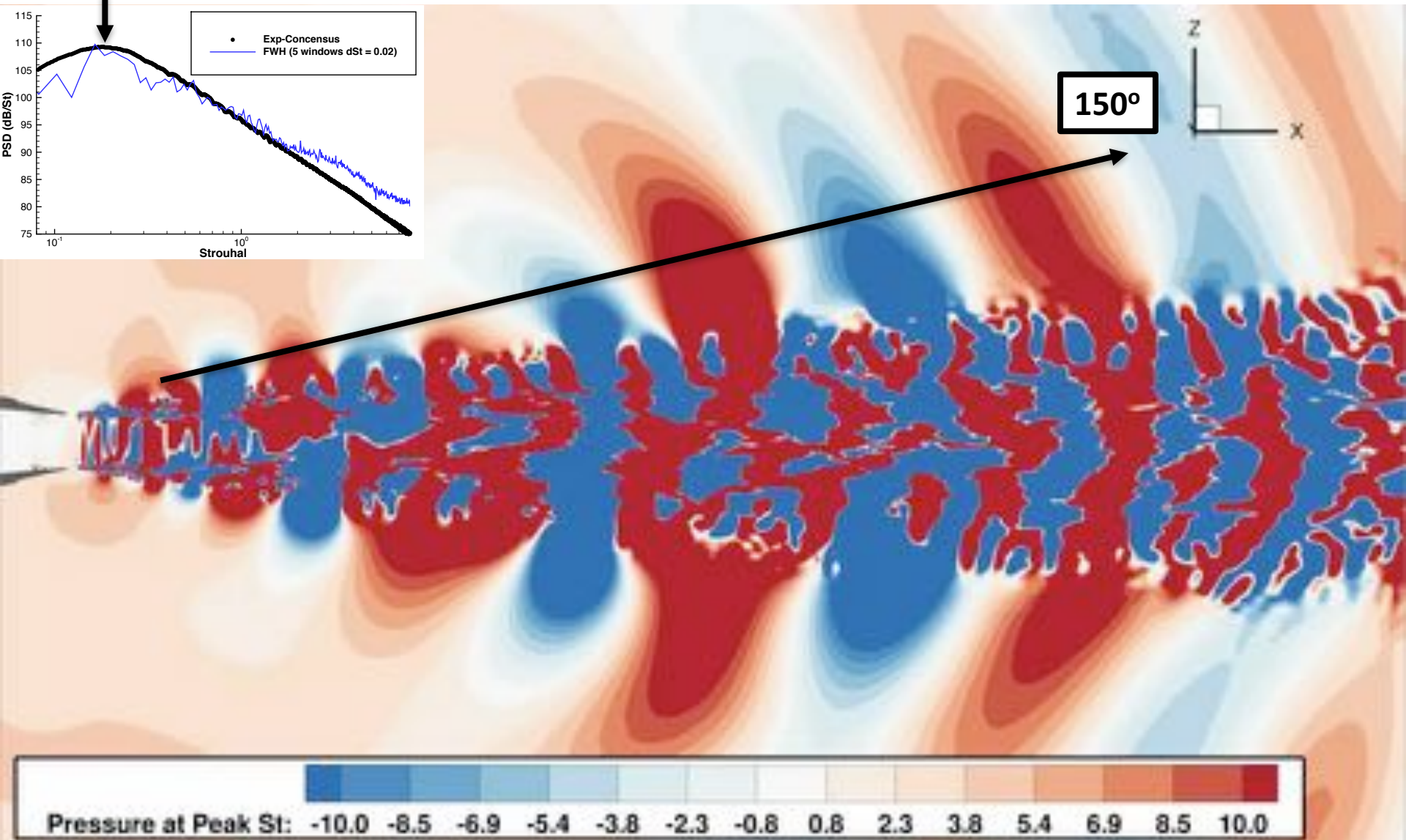
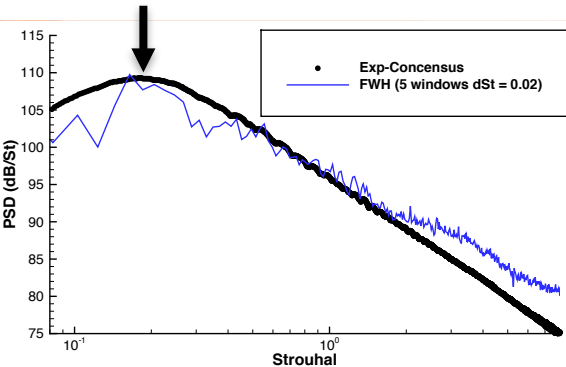
Far-Field Comparison: Band-Limited OASPL ( $0.08 \leq St \leq 8.0$ )



# Computational Results – Far-Field



Time-Domain Pressure Associated with Peak Frequency (1100Hz) in 150°



# Outline



- Introduction
- Experimental Setup
- Computational Methodology
- Structured Overset Grid System
- Computed Results
  - Near-Field Comparison
  - Far-Field Comparison
- **Summary**
- **Future Work**



# Summary



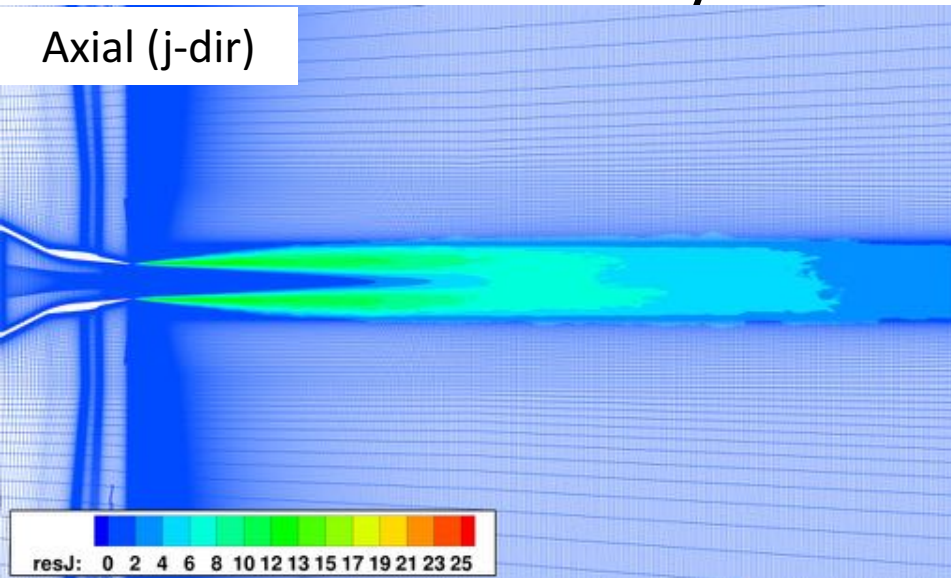
- The hybrid RANS/LES approach, within the LAVA framework, using structured curvilinear overlapping grids for the prediction of jet noise and compared our results to existing near-field PIV and far-field microphone data.
- Demonstrated improvements:
  - Hybrid RANS-NLES reduces the delay in transition to 3D turbulent structures and improved lip-line RMS prediction
  - SEM eliminates delay even further
- Completed far-field acoustic propagation
  - Mach wave radiation noise in the jet direction is well-captured
  - Sideline noise caused by turbulent fluctuations is over-predicted, likely due to elevated lip-line RMS at nozzle exit
- BL needs to be resolved better inside of nozzle for further improvements

# Future Work

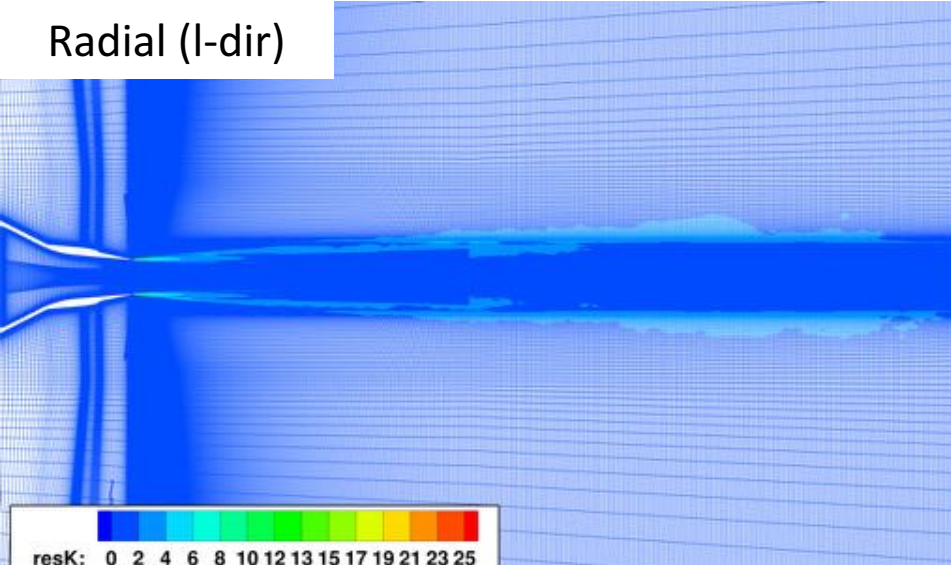


## *a Posteriori* Error Analysis

Axial (j-dir)



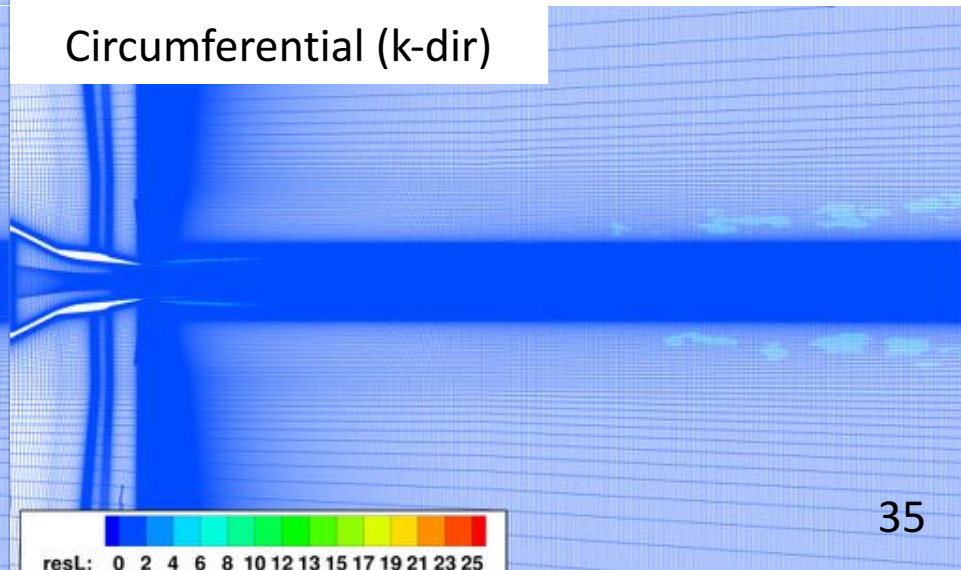
Radial (l-dir)



AIAA-2017-0978 Anisotropic grid-adaptation  
in LES of wall-bounded and free shear flows,  
Toosi and Larsson

- Analyze the difference in turbulent kinetic energy using the resolved velocity field with filtered version of resolved velocity field.
- Independent filtering in each direction leads to anisotropic measure for refinement

Circumferential (k-dir)



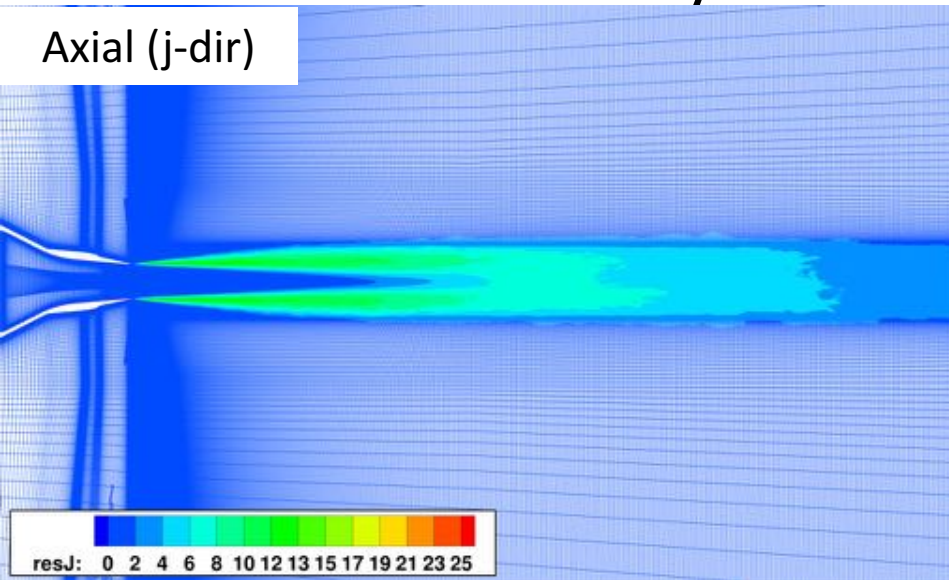


# Future Work

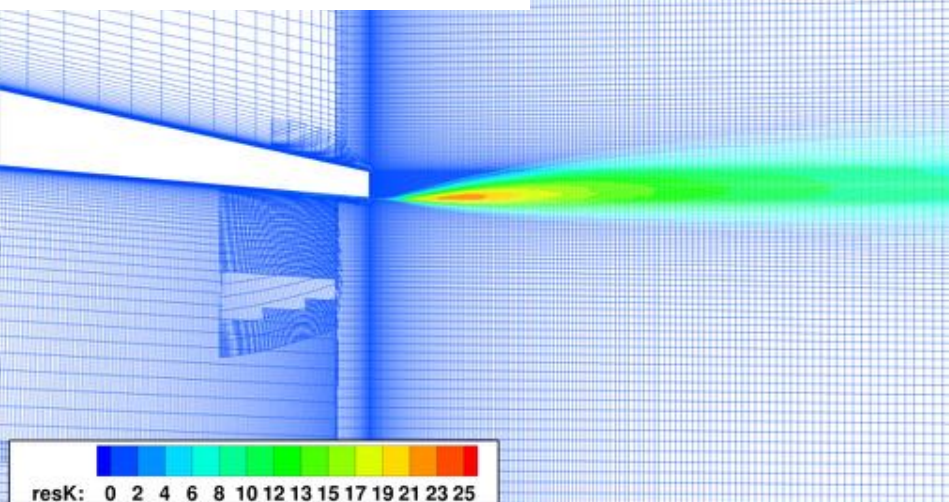


## *a Posteriori* Error Analysis

Axial (j-dir)



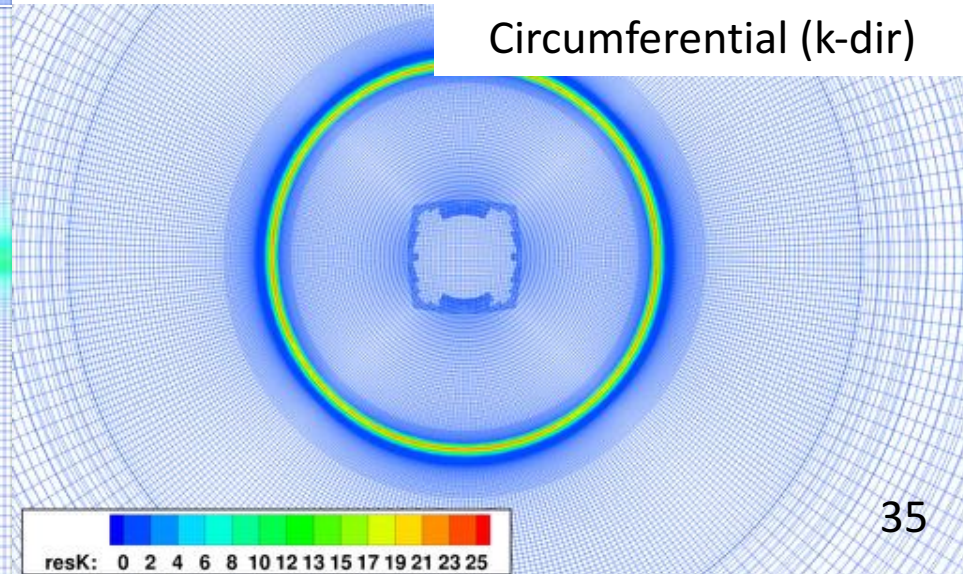
Circumferential (k-dir)



AIAA-2017-0978 Anisotropic grid-adaptation  
in LES of wall-bounded and free shear flows,  
Toosi and Larsson

- Resolution in streamwise direction is lacking the most.
- The error estimate has largest magnitude in circumferential direction.
- Radial direction pretty good.
- Improved mesh (191 M) for further investigation of SP7 and all SP3 runs

Circumferential (k-dir)



# Future Work

## LES with explicit subgrid-scale (SGS) model and SEM

**We need wall-modeled LES in order to resolve the boundary layer inside the nozzle!**

- No RANS downstream of SEM location
- Waffle cone structures inside nozzle reduced
- Artificial turbulence from SEM decays towards nozzle exit due to lack of resolution
- Recommended resolution:  
wall-resolved  $\Delta s_{circ}^+ = 20$  (12.5k points)  
wall-modeled  $\Delta s_{circ} = 0.1\delta$  (2450 points)

### QUESTION:

*"How will SGS model affect our lipline RMS and farfield solutions"*





# Acknowledgements



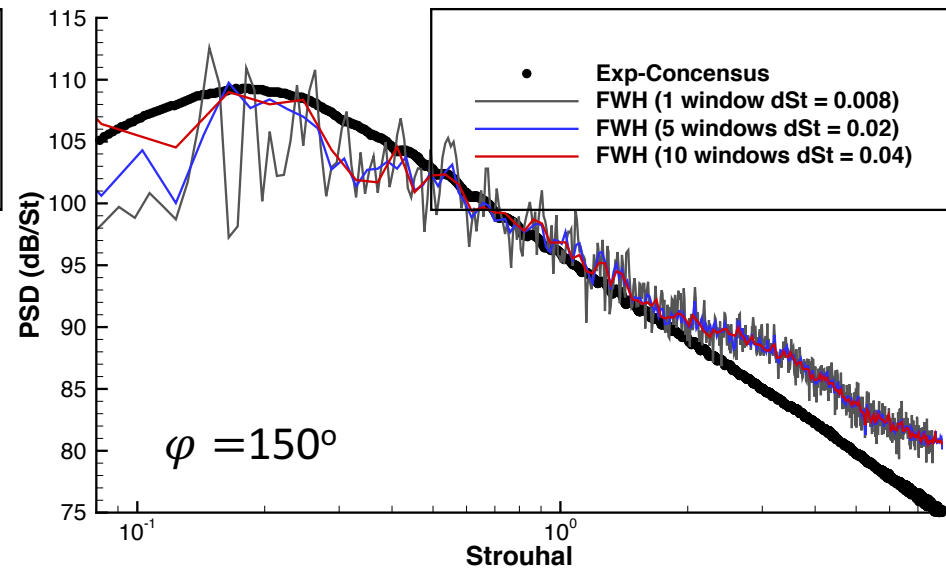
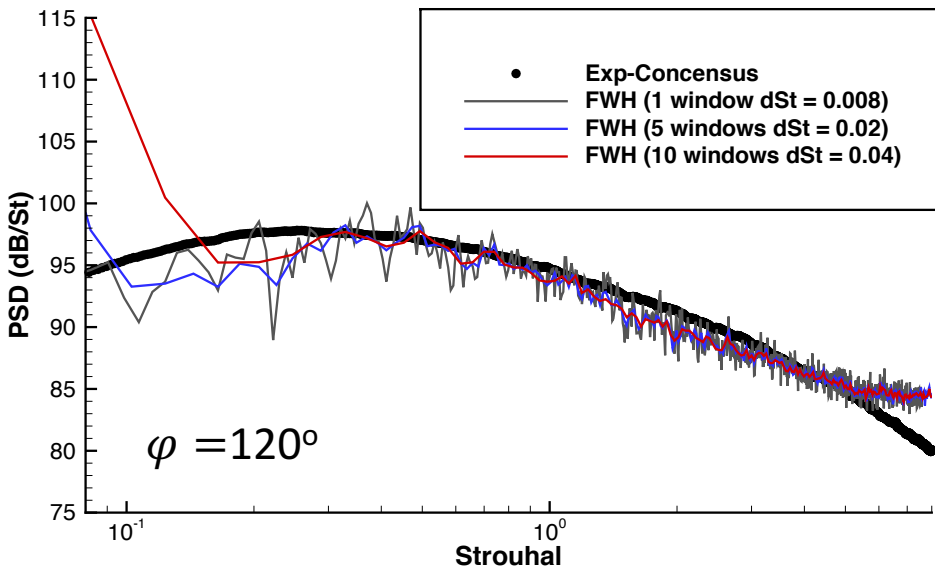
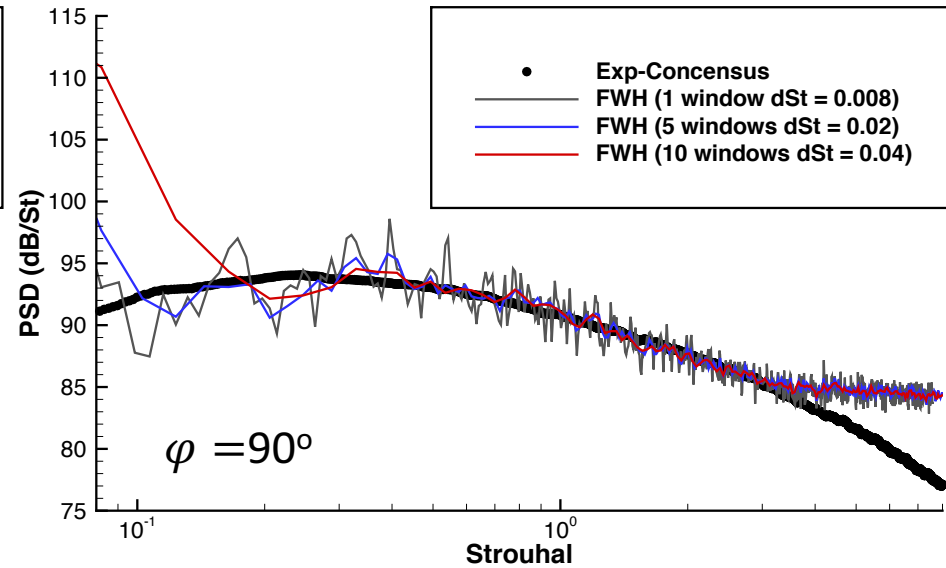
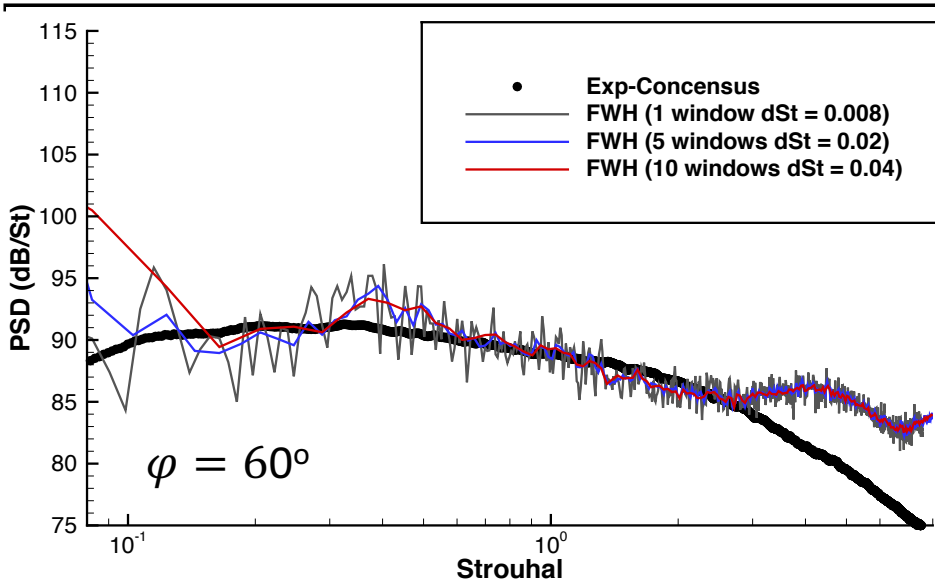
- This work was also partially funded by the Commercial Supersonics Technology (CST) project and the Transformational Tools and Technology (T<sup>3</sup>) project under the Aeronautics Research Mission Directorate (ARMD).
- Computer time has been provided by the NASA Advanced Supercomputing (NAS) facility at NASA Ames Research Center.
- Patrick J. Moran from NASA Ames visualization team for rendering of numerical schlieren video.
- Team members of LAVA group for helpful discussions and advise: Joseph George Kocheemoolayil, Francois Cadieux, Michael Barad

# Questions?

---



# Far-Field PSD



Far-Field Comparison: PSD Spectrum at 100D from exit

# Hybrid RANS/LES



## Non-Zonal model:

- DES suffers from model stress depletion (forces transition to LES but mesh too coarse to resolve field)
- DDES remains in RANS mode in attached BL. Shielding function often shows strange behavior in transition (RANS -> LES -> RANS -> LES)
- Improved length scale (Shur, Spalart, Strelet): depletes eddy viscosity faster.
- Grey-Zone-Problem: mesh fine enough to trigger 3d fluctuations in the BL, but not fine enough to resolve largest scales in BL for accurate skin-friction.

## Zonal model:

- User defines zones of RANS, LES and RANS/LES
- Numerical LES (NLES) includes wall distance and  $y^+$  based transition
- Grey-Zone-Problem is still an issue

$$f_d = 1 - \frac{1}{2} \left[ 1 - \tanh(\epsilon_d (d_{wall} - d_0)) \right]$$

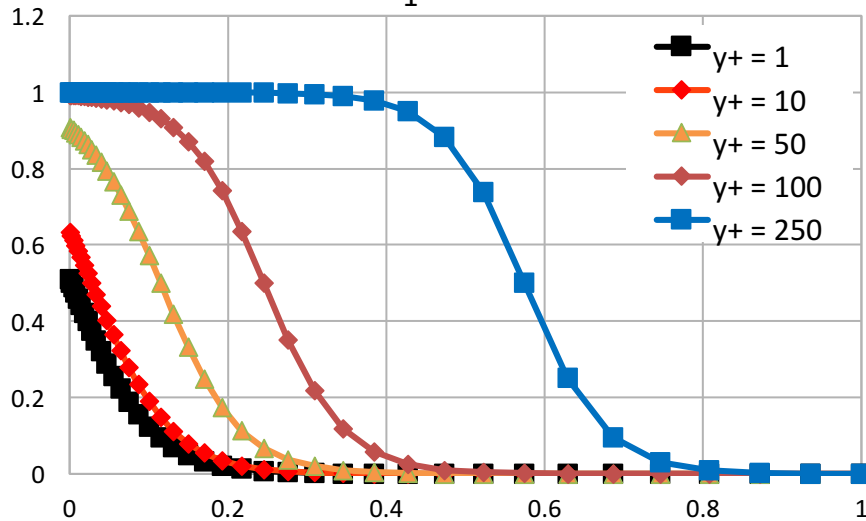
$d_{wall}$  : walldistance  
 $d_0$  : transition distance (user)  
 $\epsilon_d$  : blending (user)



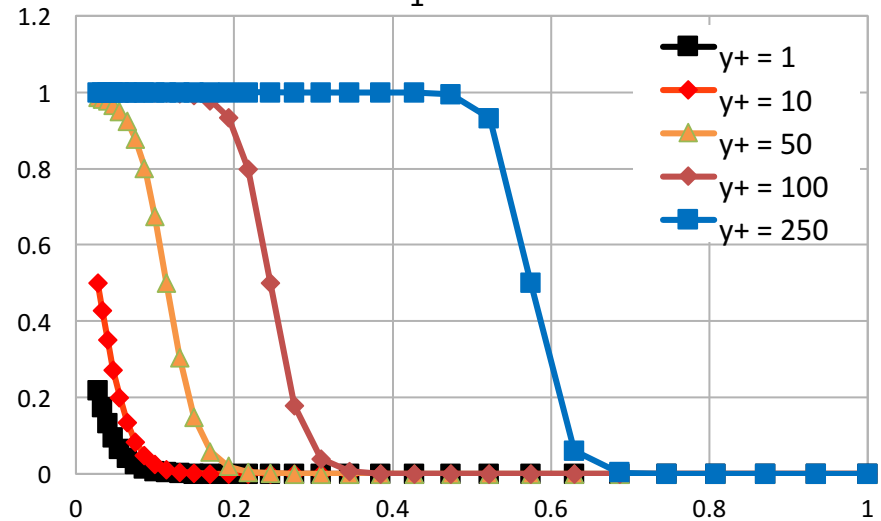
# Hybrid RANS/NLES



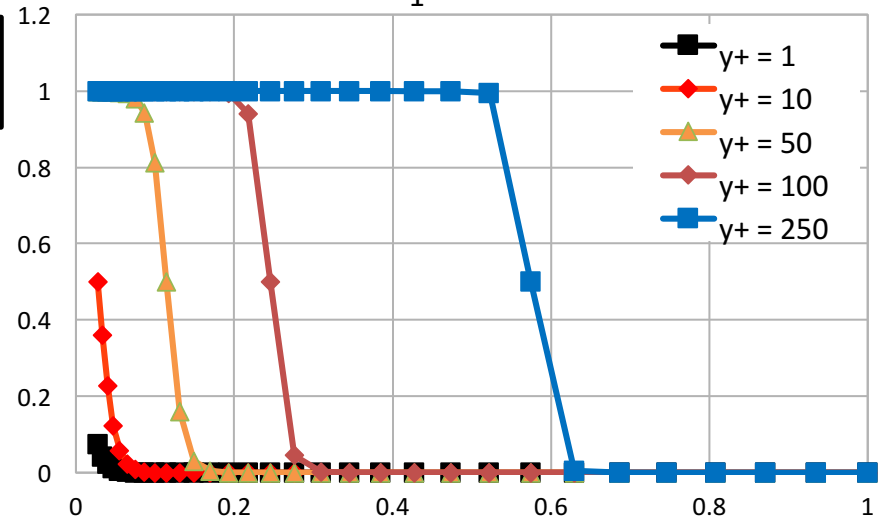
$C_1 = 10$



$C_1 = 25$



$C_1 = 50$



$$[LES/RANS] = (1 - \Gamma(\eta)) \cdot [LES] + \Gamma(\eta) \cdot [RANS]$$

$$\Gamma(\eta) = \frac{1}{2} - \frac{1}{2} \cdot \tanh [C_1 \cdot (\eta - \eta_0)]$$

$\eta$  distance from the wall

$\eta_0$  controls where the blending starts

$C_1$  controls the blending “width”

# Synthetic Eddy Method (SEM)



Jarrin, N. (2006) – A Synthetic-eddy-method for generating inflow conditions for LES

1. Define a Box of eddies with:

$$x_{j,min} = \min_{\mathbf{x} \in S} (x_j - \sigma_{ij}(\mathbf{x})) \quad x_{j,max} = \max_{\mathbf{x} \in S} (x_j + \sigma_{ij}(\mathbf{x}))$$

2. Generate for each eddy  $k$  random vectors for the location  $\mathbf{x}^k$  and intensity  $\epsilon^k$

3. Compute the velocity signal on the set of Points  $S$  with:

$$u_i = U_i + \frac{1}{\sqrt{N}} \sum_{k=1}^N a_{ij} \epsilon^k f_{\sigma_{ij}} (x - x^k)$$

$$f_{\sigma_{ij}} (x - x^k) = \sqrt{V_b} \cdot \frac{1}{\sigma_{i1}} f \left( \frac{x_1 - x_1^k}{\sigma_{i1}} \right) \cdot \frac{1}{\sigma_{i2}} f \left( \frac{x_2 - x_2^k}{\sigma_{i2}} \right) \cdot \frac{1}{\sigma_{i3}} f \left( \frac{x_3 - x_3^k}{\sigma_{i3}} \right)$$

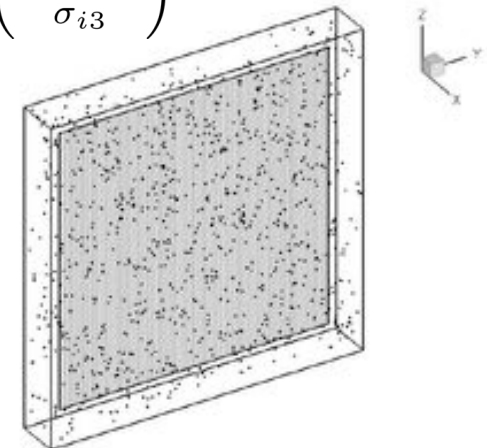
$$f(x) = \begin{cases} \sqrt{\frac{3}{2}} (1 - |x|) & x < 1 \\ 0 & else \end{cases}$$

4. Convect the eddies through  $B$  with velocity  $U_{ref}$

$$x^k(t + dt) = x^k(t) + U_{ref} \cdot dt$$

5. Generate new locations  $\mathbf{x}_k$  and intensities for eddies which were convected out of  $B$ .

Advance to next time step and go back to step 3



# Launch Ascend and Vehicle Aerodynamics (LAVA)

